© 2021. Published by The Company of Biologists Ltd | Journal of Cell Science (2021) 134, jcs258922. doi:10.1242/jcs.258922

RESEARCH ARTICLE

The role of USP7 in the Shoc2-ERK1/2 signaling axis and Noonan-like syndrome with loose anagen hair

Patricia Wilson, Lina Abdelmoti, Rebecca Norcross, Eun Ryoung Jang, Malathy Palayam and Emilia Galperin*

ABSTRACT

The ERK1/2 (also known as MAPK3 and MAPK1, respectively) signaling pathway is critical in organismal development and tissue morphogenesis. Deregulation of this pathway leads to congenital abnormalities with severe developmental dysmorphisms. The core ERK1/2 cascade relies on scaffold proteins, such as Shoc2 to guide and fine-tune its signals. Mutations in *SHOC2* lead to the development of the pathology termed Noonan-like Syndrome with Loose Anagen Hair (NSLAH). However, the mechanisms underlying the functions of Shoc2 and its contributions to disease progression remain unclear. Here, we show that ERK1/2 pathway activation triggers the interaction of Shoc2 with the ubiquitin-specific protease USP7. We reveal that, in the Shoc2 module, USP7 functions as a molecular 'switch' that controls the E3 ligase HUWE1 and the HUWE1-induced regulatory feedback loop. We also demonstrate that disruption of Shoc2-USP7 binding leads to aberrant activation of the Shoc2-ERK1/2 axis. Importantly, our studies reveal a possible role for USP7 in the pathogenic mechanisms underlying NSLAH, thereby extending our understanding of how ubiquitin-specific proteases regulate intracellular signaling.

KEY WORDS: ERK1/2, HUWE1, USP7, Shoc2 scaffold, RASopathy

INTRODUCTION

Noonan-like syndrome with loose anagen hair (NSLAH; OMIM, 607721) is one of the developmental disorders characterized by dysregulation of the extracellular signal-regulated kinases 1 and 2 (ERK1/2, also known as MAPK3 and MAPK1, respectively) signaling pathway (Tidyman and Rauen, 2016). Cumulatively called RASopathies, these developmental diseases present with a spectrum of overlapping symptoms (Tidyman and Rauen, 2016). NSLAH is caused by hereditary mutations in the *SHOC2* gene that codes for a positive regulator of the ERK1/2 pathway, the scaffold protein Shoc2. Patients harboring mutations in the *SHOC2* gene present with a number of congenital defects, including facial dysmorphia (e.g. ocular hypertelorism), cleft palate, cardiac abnormalities and short stature (Baldassarre et al., 2014; Choi et al., 2015; Cordeddu et al., 2009; Couser et al., 2018; Gargano et al., 2014; Lo et al., 2015).

Studies over the past decade have uncovered the critical role of the Shoc2 scaffold in the transmission of signals through the core ERK1/2 cascade (Jang et al., 2021). These studies convincingly demonstrated that this seemingly auxiliary component of the ERK1/2 signaling network is an indispensable regulator of the ERK1/2 pathway, as its loss was shown to have a profound effect on the development of several organisms, including *Caenorhabitis. elegans* (Sieburth et al., 1998), zebrafish (Jang et al., 2019b) and mice (Yi et al., 2010). The molecular mechanisms by which this non-enzymatic scaffold coordinates transmission of ERK1/2 signals rely on its ability to build intricate multiprotein machinery (Jang et al., 2021). Shoc2 tethers m-RAS, RAF-1 and the catalytic subunit of protein phosphatase 1c (PP1c, also known as PPP1CA) to accelerate ERK1/2 signals (Rodriguez-Viciana et al., 2006; Young et al., 2013). Shoc2 also recruits a number of proteins of the ubiquitin machinery to fine-tune signals transmitted via the module.

Our earlier studies demonstrated that activation of the ERK1/2 pathway triggers Shoc2 and RAF-1 ubiquitylation by the E3 ligase HUWE1 (Jang et al., 2014). This HUWE1-mediated ubiquitylation is used as a negative-feedback mechanism that modulates the ability of the scaffold to accelerate the signaling activity of the ERK1/2 pathway (Jang et al., 2014). In turn, the (AAA+) ATPases PSMC5 and VCP/p97 modulate the HUWE1-modified Shoc2 and RAF-1 ubiquitylation by remodeling the scaffold complex in a spatially controlled manner (Jang et al., 2019a). An additional E3 ligase, FBXW7, has also been implicated in the ubiquitylation of Shoc2 (Xie and Sun, 2019). However, unlike HUWE1, the E3 ligase FBXW7 appears to be involved in balancing ERK1/2 and MTOR signals for cell proliferation and autophagy (Xie et al., 2019). Although proteins of the ubiquitin machinery have been shown to differentially interact with wild-type or mutant Shoc2 (Jang et al., 2015), a complete picture of the Shoc2 interactome is lacking. There is also no clear understanding of whether changes in Shoc2 interactions with the proteins of ubiquitin machinery can explain the pathogenesis of NSLAH.

Protein ubiquitylation is one of the best-studied post-translational modifications (Kwon and Ciechanover, 2017). Its important role in a variety of cellular functions via the regulation of protein stability and activity has been established by vast numbers of studies. Consequently, the accurate trimming of ubiquitin marks by de-ubiquitylating enzymes (DUBs) is also an essential process for many cellular functions (Basar et al., 2021). Moreover, cooperativity between these two counterbalancing activities, ubiquitylation and de-ubiquitylation, appears to be critical for the control of cellular signaling yet is not fully understood. In this study, we hypothesize that the transient nature of Shoc2 ubiquitylation suggests a de-ubiquitylating enzyme is intimately involved in the modulation of HUWE1-induced Shoc2/RAF-1 ubiquitylation, and is potentially involved in the pathophysiology of NSLAH.

Here, we identified the de-ubiquitylating enzyme USP7 as a novel component of the Shoc2 signaling complex. USP7, frequently referred to as herpes virus-associated ubiquitin-specific protease (HAUSP), is a member of the ubiquitin-specific protease (USP) subgroup of DUBs. USP7 is known for its role in controlling the

Department of Molecular and Cellular Biochemistry, University of Kentucky, Lexington, KY 40536, USA.

*Author for correspondence (emilia.galperin@uky.edu)

E.G., 0000-0002-8743-026X

Handling Editor: Daniel Billadeau
Received 18 May 2021; Accepted 9 September 2021

Journal of Cell Science (2021) 134, jcs258922. doi:10.1242/jcs.258922

function and stability of proteins, such as p53, MDM2 and Myc (Nicklas et al., 2019; Sheng et al., 2006). It is also known for its propensity to form stable complexes with many of its partners, of which a surprisingly large number are E3 ligases (Kim and Sixma, 2017). The USP7-E3 interaction was shown to protect E3 ligases from auto-ubiquitylation leading to predominant E3 ligase activity (Ma et al., 2014; Nathan et al., 2008). USP7 hence works as a 'switch' that can shift its activity from the E3 ligase to the target, thus allowing for degradation of the E3 ligase and the protection of the target (Kim and Sixma, 2017).

We found that USP7 interacts with Shoc2 and HUWE1 in response to EGF-induced activation of the ERK1/2 pathway. In the Shoc2 complex, USP7 regulates the HUWE1-mediated negative feedback loop that modulates the amplitude of Shoc2-ERK1/2 signals. The present study dissects the Shoc2-USP7-HUWE1 interactions on a biochemical level and provides evidence that, by binding to the Shoc2 scaffold, USP7 forms a USP7-Shoc2-HUWE1 molecular switch and creates a rapid response within the pathway. USP7 knockdown, loss of its activity, or its inability to recognize the Shoc2 scaffold, disrupt signal transmission via the Shoc2-ERK1/2 signaling axis. Importantly, our findings demonstrate differential binding of Shoc2 NSLAH variants to USP7, and implicate the USP7 de-ubiquitylase broadly in the pathogenesis of NSLAH RASopathy.

RESULTS

Shoc2 mutations associated with developmental pathologies show aberrant ubiquitylation

NSLAH is associated with distinct missense mutations in the *SHOC2* gene. The most commonly identified NSLAH pathogenic variant is the Shoc2 ($S^{2}G$) substitution (Cordeddu et al., 2009). Other reported NSLAH variants include $M^{173}I$ (Hannig et al., 2014) and $QH^{269/270}HY$ (Hannig et al., 2014; Motta et al., 2019). Our queries of the publicly available Database of Genomic Variation and Phenotype in Humans using Ensembl Resources (DECIPHER, Firth et al., 2009) identified a case with heterozygous chromosomal microdeletions (see Fig. 1A and Table S1 for genomic coordinates) and six cases with a heterozygous missense mutation in Shoc2 (Fig. 1A). Subsequent analysis revealed three new Shoc2 mutations ($E^{89}D$, $C^{238}Y$ and $L^{473}I$) that were not reported as NSLAH-causing mutations. Therefore, we obtained available detailed clinical information on the affected individuals in a genotype-to-phenotype approach (Tables S1, S2). All of these individuals exhibited a striking overlap with the clinical phenotypes observed in NSLAH patients: notably, craniofacial dysmorphisms, optic atrophy, cardiovascular abnormalities, alterations in limbic and nervous systems, cleft palate and developmental delays. The most prevalent phenotypes, such as heart defects, intellectual disability, short stature, hair loss and skin tags indicated possible pathogenicity of these Shoc2 variants.

Next, we examined whether the newly identified Shoc2 variants ($E^{89}D$, $C^{238}Y$ and $L^{473}I$) could support ERK1/2 signals when expressed in the Shoc2 CRISPR knockout HeLa cells (Fig. 1B; Fig. S1A,B). Data in Fig. 1B,C show that Shoc2 pathogenic variants $Shoc2^{E89D}$, $Shoc2^{QH269/270HY}$ and $Shoc2^{L473I}$ were not able to fully rescue ERK1/2 phosphorylation. Our earlier studies also found that Shoc2-ERK1/2 signals are fine-tuned by non-proteolytic ubiquitylation of Shoc2 (Jang et al., 2014, 2019a) and demonstrated differences in the levels of ubiquitylation of wild-type Shoc2 and the Shoc2 ($S^{2}G$) NSLAH mutant (Jang et al., 2015). Thus, we tested the levels of ubiquitylation for each Shoc2 variant in Shoc2 knockout cells and found that Shoc2 variants $L^{473}I$, $QH^{269/270}HY$ and $S^{2}G$ had elevated levels of ubiquitylation (Fig. 1D,E). Interestingly, the protein half-life of the Shoc2 mutants was comparable to that of wild-type Shoc2 (Fig. S1C).

To physiologically assess the Shoc2 variants that presented with increased levels of ubiquitylation, we used the zebrafish vertebrate model. Zebrafish have emerged as an excellent model for interrogating developmental mutations (Jindal et al., 2015, 2017). The *Danio rerio* genome encodes a single Shoc2 ortholog that is highly homologous to human Shoc2 at the amino acid level, sharing 88.5% identity (Jeoung et al., 2013). The loss of Shoc2 in zebrafish leads to a profound deficiency of circulating blood cells, likely due to defects in both primitive and definitive waves of hematopoiesis and underdeveloped vascularization (Jang et al., 2019a). Thus, we evaluated the pathogenicity of the Shoc2 variants with increased levels of ubiquitylation and 100% conserved in at least nine Shoc2 orthologs, including *Danio rerio* (Jeoung et al., 2013), by comparing the ability of wild-type Shoc2 and Shoc2 harboring S2G, L437I and QH269/270YH substitutions to rescue defects in erythropoiesis of zebrafish embryos depleted of Shoc2.

As we demonstrated previously, embryos injected with *shoc2* morpholino (MO) almost completely lacked *o*-Dianisidine staining detecting hemoglobin of erythropoietic cells in the ducts of Cuvier, over the yolk sac and tail compared to the embryos injected with control morpholino (cMO) (Jang et al., 2019b) (Fig. 2A-C). Yet, embryos injected with wild-type *shoc2* zebrafish mRNA rescued the *shoc2* MO-induced defects in erythrocyte circulation. In contrast, embryos injected with *shoc2* mRNA harboring $Shoc2^{S2G}$, $Shoc2^{L437I}$ or $Shoc2^{QH269/270YH}$ mutations did not rescue early erythropoiesis to the level of wild-type Shoc2. The examination of differences in the rescue was highly significant (χ^{2} analysis), supporting our observations in Fig. 2A,B. Noteworthy, ectopic expression of the NLSAH $S^{2}G$, $QH^{269/270}HY$ and the $L^{473}I$ Shoc2 variants also resulted in poor survival of injected embryos compared to wild-type mRNA injections. These observations indicate that similarly to $Shoc2^{S2G}$ and $Shoc2^{QH269/270HY}$, the $Shoc2^{L437I}$ variant is likely to be NSLAH causative, with developmental defects similar to those observed in patients carrying $Shoc2^{S2G}$ and $Shoc2^{QH269/270HY}$ mutations. Together, data in Figs 1, 2 indicate that $L^{473}I$, $QH^{269/270}HY$ and $S^{2}G$ substitutions possibly affect mechanisms that regulate the non-proteolytic ubiquitylation of Shoc2 thereby affecting Shoc2 function.

USP7 interacts with and de-ubiquitylates Shoc2

None of the NSLAH-associated Shoc2 variants with increased protein ubiquitylation were in the HUWE1-binding domain of Shoc2 (Jang et al., 2014), suggesting that Shoc2-HUWE1 interaction is not affected. Thus, we set out to identify a peptidase that regulates the deubiquitylation of Shoc2. A member of the USP subgroup of deubiquitylating enzymes, USP7, also referred to as HAUSP, has been previously functionally linked to HUWE1 (Besche et al., 2009; Khoronenkova and Dianov, 2013; Sowa et al., 2009). To evaluate whether a deficiency in USP7 leads to the excessive ubiquitylation of the Shoc2 mutants, we examined whether USP7 could be associated with the Shoc2 scaffolding complex. First, we examined the interaction of glutathione S-transferase (GST)-fused Shoc2 (GST-Shoc2) with Flag-tagged USP7 (FLAG-USP7) or Myc-tagged USP46 (Myc-USP46) that belongs to the same subgroup of DUBs as USP7 (Li et al., 2013). Co-immunoprecipitation experiments using exogenously expressed proteins showed that only USP7 specifically interacts with Shoc2 in HEK-293 cells (Fig. 3A). Interaction of endogenous Shoc2-USP7

Journal of Cell Science (2021) 134, jcs258922. doi:10.1242/jcs.258922

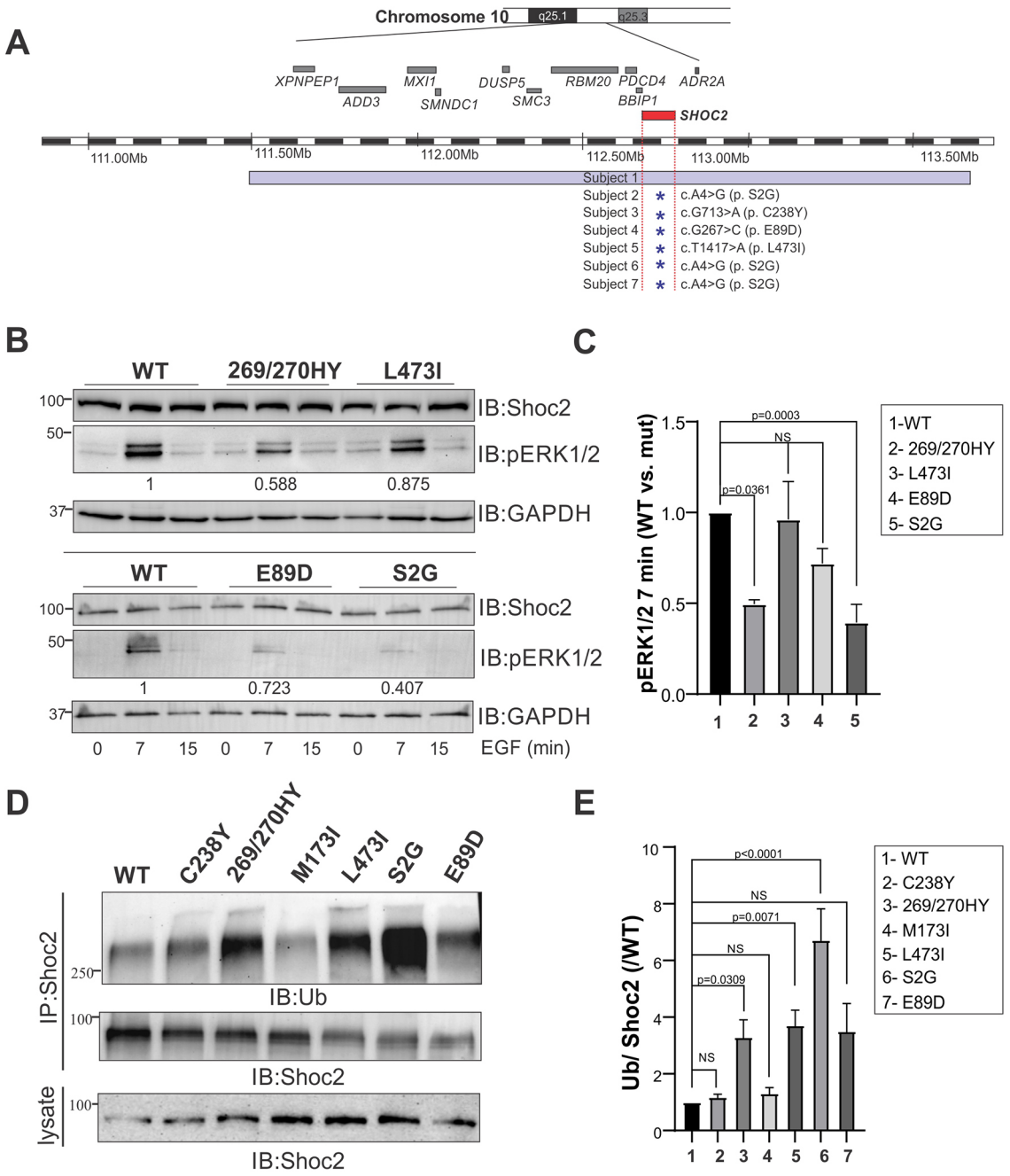

Fig. 1. Shoc2 variants identified in patients with NSLAH-related phenotypes. (A) Schematic of the *SHOC2* genomic locus in which deletion or mutations in seven subjects with NSLAH phenotypes were identified (see Table S1). Red line and asterisks indicate the position of the *SHOC2* gene. (B) The Shoc2 NSLAH variants differentially regulate ERK1/2 phosphorylation. HeLa Shoc2 CRISPR knockout cells transiently transfected with the Shoc2 NSLAH mutants were serum starved for 16 h and then stimulated with EGF (0.2 ng/ml) for 7 and 15 min. Cell lysates were analyzed using anti-pERK1/2, -GAPDH and -Shoc2 antibodies. (C) Bar graph showing the mean amount of pERK1/2 in cells expressing Shoc2 mutants normalized to the total amount of GAPDH in arbitrary units compared to cells expressing wild-type (WT) Shoc2-tRFP at 7 min±s.e. (n=4) [P=0.036 (269/270HY), P=0.0003 (S2G), NS (not significant) (L437I and E89D), Kruskal–Wallis test]. The results in each panel are representative of four independent experiments. (D) Ubiquitylation of Shoc2 variants identified in patients with NSLAH-related phenotypes. CRISPR/Cas9 Shoc2 knockout HeLa cells were transfected with the indicated Shoc2-tRFP mutants. Shoc2 was then precipitated from denatured cell lysates using an anti-Shoc2 antibody. Immunoblots (IB) were analyzed with anti-Shoc2 and anti-ubiquitin (Ub) antibodies. The results in each panel are representative of at least three independent experiments. (E) Bar graph showing the mean amount of ubiquitin normalized to the total amount of Shoc2 protein compared to the ubiquitin levels of wild-type Shoc2 in arbitrary units±s.e. (n=7) (Kruskal–Wallis test, P<0.05 is reported). IP, immunoprecipitate.

was readily detected in 293FT and Cos1 cells, which further supported Shoc2-USP7 interaction (Fig. 3B).

To establish whether a USP7-Shoc2 interaction is mediated by HUWE1, we examined the binding of recombinant Shoc2 and USP7 purified from *Escherichia coli*. The Shoc2 pulldown analysis showed that Shoc2 binds USP7 in the absence of HUWE1, indicating a direct Shoc2-USP7 interaction (Fig. 3C). This finding was also validated by immunoprecipitation experiments using 293FT cells that were depleted of HUWE1 via siRNA (Fig. 3D). The loss of HUWE1 did not affect the amount of USP7 in the Shoc2 precipitates, indicating that the E3 ligase HUWE1 is not required for Shoc2-USP7 binding.

Journal of Cell Science (2021) 134, jcs258922. doi:10.1242/jcs.258922

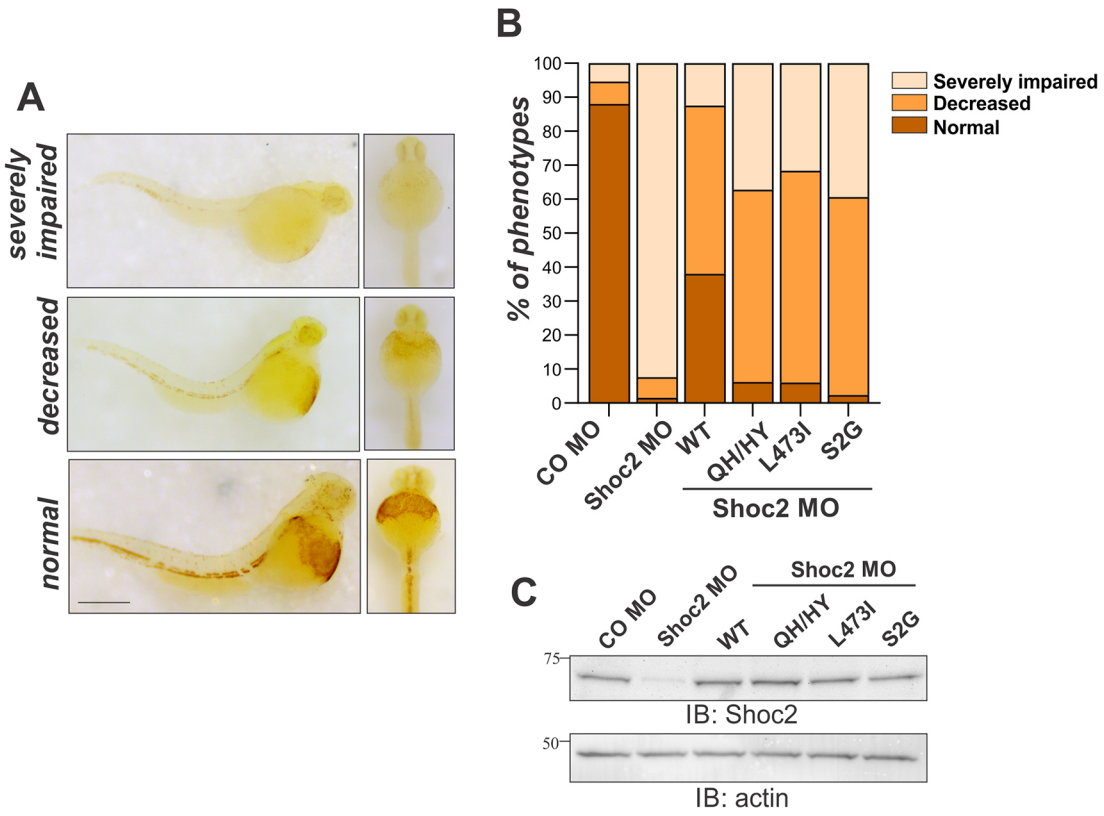

Fig. 2. Shoc2 NSLAH-related variants do not fully rescue impaired hematopoiesis of *shoc2* morphant larvae. (A) The panels show three distinct levels of hemoglobin detected by *o*-Dianisidine staining at 52 h post fertilization. Images are shown in lateral and ventral view. (B) The rescue effect of ectopic shoc2 mRNA expression in the shoc2 morphants. The bar graph shows the ratio of various rescue effects following injection with shoc2 MO, shoc2 mRNA and their combination. Relative intensity of hemoglobin staining was scored in arbitrary units of intensity (a.u.i.) 1 to 3, 1 being the weakest and 3 the strongest. The percentage by class is significantly different (P<0.0001, χ^2 analysis) for Shoc2 MO co-injections with Shoc2 mRNAs for the S2G, 269/270QH and L473I variants compared with Shoc2 MO co-injections with Shoc2 wild-type (WT) mRNA (χ^2 value wild type versus 269/270QH=94.94, d.f.=2, P<0.001; wild type versus L473I=48.23,94, d.f.=2, P<0.001; wild type versus S2G=64.97, d.f.=2, P<0.001; Shoc2 MO versus Shoc2 MO plus wild type=197.20, d.f.=2, P<0.001). (C) Embryos injected with *shoc2* and control MO, and indicated mRNA, were harvested for immunoblotting (IB) at 52 h post fertilization. The protein levels were analyzed using specific Shoc2 and actin antibodies. Scale bar: 500 µm.

Next, we defined a region in USP7 responsible for its recognition by Shoc2. USP7 contains a catalytic peptidase domain, an N-terminal meprin and TRAF homology (MATH) or a tumor necrosis factor receptor-associated factor (TRAF)-like domain, as well as five ubiquitin-like (UbL) domains in its C-terminal region (Fig. S2A). Through a series of co-immunoprecipitation experiments with USP7 truncations, we found that Shoc2 interacts with two distinct interfaces of USP7, the N-terminal TRAF domain and the C-terminal UbL regulatory domains (Fig. S2B). *In vitro* binding studies using recombinant Shoc2 and USP7 domains supported that both TRAF-like and UbL domains of USP7 interact with Shoc2 (Fig. S2C). Together, these data convincingly demonstrate that USP7 and Shoc2 form a complex, and establish a premise to investigate the role of USP7 in regulating ubiquitylation levels of Shoc2 and consequently ERK1/2 signaling on a molecular level.

USP7 controls Shoc2 ubiquitylation

As the best understood function of de-ubiquitylating peptidases is to stabilize their target proteins, we next examined whether the protein levels of Shoc2 or its binding partner RAF-1 are controlled by USP7. Treatment with USP7 inhibitors P22077 or HBX41108 (Fig. S3A,B,D) did not affect the protein levels of Shoc2, RAF-1 or HUWE1 in HeLa, 293FT or Cos1 cells, indicating that USP7 is unlikely to control the turnover of either Shoc2 or its partners RAF-1 and HUWE1. Similarly, we did not observe a change in the levels of the E3 ligase HUWE1 or Shoc2 when cells were siRNA depleted of USP7 (Fig. S3C). Yet, when assessing the ubiquitylation of Shoc2 in cells depleted of USP7 using denaturing conditions to prevent the detection of other ubiquitylated proteins in the complex, we observed a marked increase (Fig. 3E). A similar increase in Shoc2 ubiquitylation was found in cells treated with USP7 inhibitors P22077 (Fig. 3F) and HBX41108 (Fig. S4A). Moreover, ectopic expression of the enzymatically inactive USP7 mutant (USP-C223S), but not wild-type USP7, led to a moderate increase in Shoc2 ubiquitylation (Fig. S4B). Importantly, the ubiquitylation level of RAF-1 was also dramatically increased in cells treated with the USP7 inhibitor P22077 (Fig. S4C). Together, these observations suggest that USP7 regulates the level of ubiquitylation on Shoc2 and RAF-1 but not their stability.

USP7 modulates HUWE1-mediated fine-tuning of the Shoc2-ERK1/2 signaling axis

Previously, we demonstrated that epidermal growth factor (EGF)-induced activation of the ERK1/2 pathway stimulates HUWE1-mediated ubiquitylation of Shoc2 (Jang and Galperin, 2016; Jang et al., 2019a). Thus, we examined whether USP7 affects the amplitude of the EGF-induced Shoc2 ubiquitylation (Fig. 4A,B). In cells treated with the USP7 inhibitor P22077 and then stimulated with EGF (Fig. 4A, lanes 1-4), the amplitude of Shoc2

Journal of Cell Science (2021) 134, jcs258922. doi:10.1242/jcs.258922

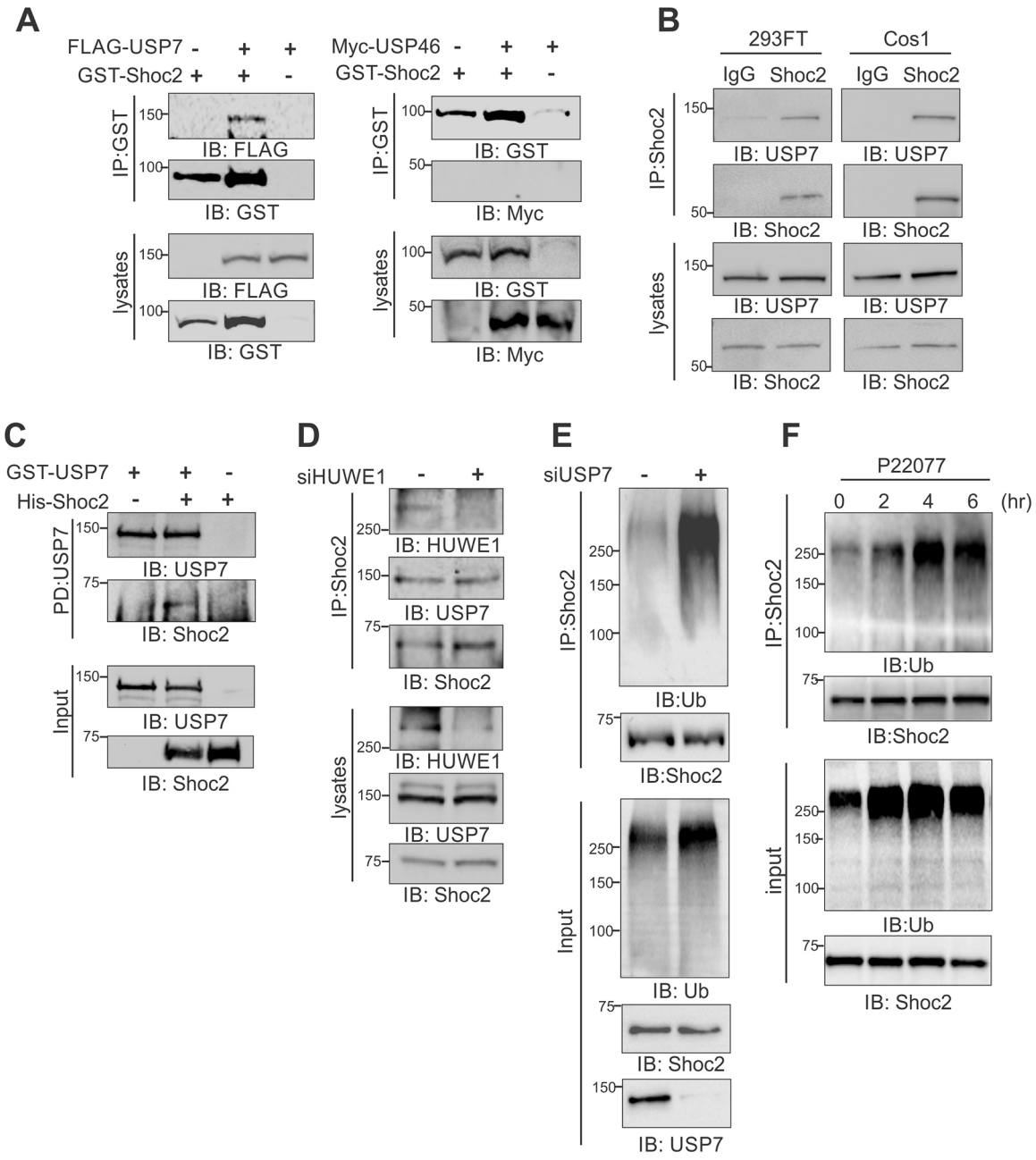

Fig. 3. USP7 interacts with Shoc2 and modulates Shoc2 ubiquitylation. (A) The 293FT cells were co-transfected with GST-Shoc2, FLAG-USP7 or Myc-USP46. GST-Shoc2 was immunoprecipitated (IP) using GST antibody and analyzed by immunoblotting (IB) using anti-MYC, -FLAG or -GST antibodies. (B) Endogenous Shoc2 was immunoprecipitated from 293FT and Cos1 cells using Shoc2 antibody. Anti-USP7 antibodies were used to detect USP7 in Shoc2 immunoprecipitates and in total cell lysates. (C) Recombinant His-Shoc2 was mixed with GST-USP7 coupled to glutathione Sepharose beads. Complexes were analyzed using anti-Shoc2 and -USP7 antibodies. (D) Endogenous Shoc2 was immunoprecipitated from 293FT cells transiently transfected with non-targeting siRNA (siNT) or HUWE1 siRNA (siHUWE1) using anti-Shoc2 antibody. The immunoprecipitates were analyzed with anti-HUWE1, -USP7 and -Shoc2 antibodies. The results in each panel are representative of three independent experiments. (E) Endogenous Shoc2 was immunoprecipitated from 293FT cells transiently transfected with non-targeting siRNA (siNT) or USP7 siRNA (siUSP7). The immunoprecipitates were analyzed by immunoblotting using anti-Ub and -Shoc2 antibodies. Cell lysates were analyzed using anti-USP7, -Ub and -Shoc2 antibodies. (F) Endogenous Shoc2 was immunoprecipitated from 293FT cells treated with USP7 inhibitor P22077. Shoc2 ubiquitylation was detected by immunoblotting using anti-Ub antibody. The immunoprecipitates and cell lysates were analyzed by immunoblotting using anti-Ub and -Shoc2 antibodies. The results in each panel are representative of three independent experiments.

ubiquitylation was markedly increased compared to EGF-induced ubiquitylation of Shoc2 control cells (Fig. 4A, lanes 5-8). The EGF-induced Shoc2 ubiquitylation closely followed the ERK1/2 phosphorylation curve in the control cells, as well as in cells treated with the USP7 inhibitor. Importantly, the increased levels of Shoc2 ubiquitylation seen in cells treated with P22077 coincided with attenuated ERK1/2 phosphorylation. These findings are entirely consistent with the previously understood role of Shoc2 ubiquitylation being a part of a negative-feedback mechanism that fine-tunes EGF-induced ERK1/2 phosphorylation (Jang et al., 2014, 2019a).

Next, we assessed the activation of the Shoc2-coupled RAF-1 kinase and examined RAF-1(Ser338) phosphorylation in Shoc2 immunoprecipitates (Fig. 4C). P22077 treatment abrogated a 3-fold

Journal of Cell Science (2021) 134, jcs258922. doi:10.1242/jcs.258922

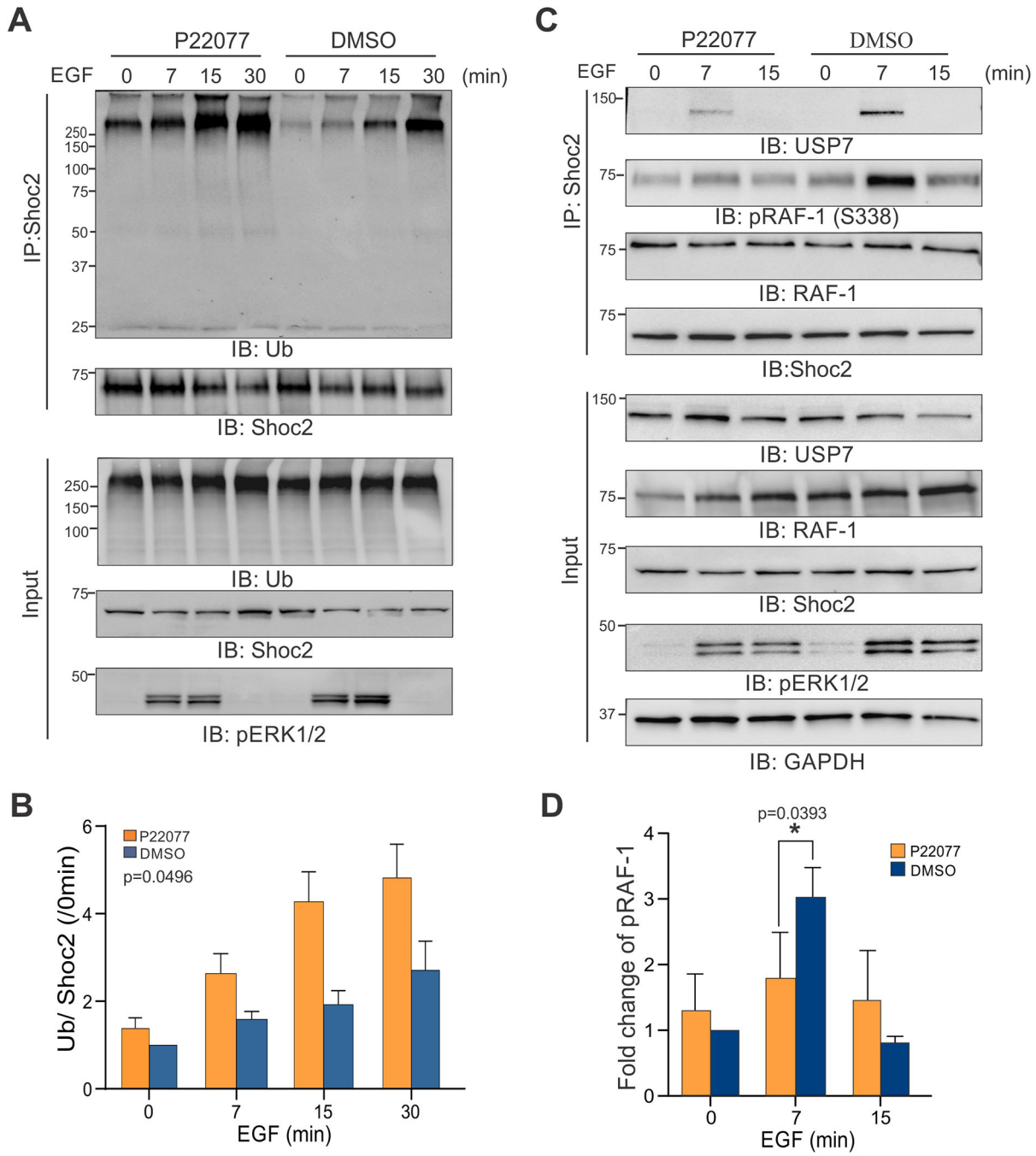

Fig. 4. USP7 modulates Shoc2 ubiquitylation and affects RAF-1/ERK1/2 activation stimulated by EGF. (A) The 293FT cells were serum starved for 16 h, treated with USP7 inhibitor P22077 (25 µM) for 4 h and then stimulated with EGF (0.2 ng/ml) for 7, 15 and 30 min. Endogenous Shoc2 was immunoprecipitated (IP) under denaturing conditions using Shoc2 antibodies. Shoc2 ubiquitylation was detected by immunoblotting (IB) using anti-Ub antibody. The immunoprecipitates and cell lysates were analyzed by immunoblotting with anti-Ub, -Shoc2 and pERK1/2 antibodies. (B) The mean amount of Ub normalized to the total amount of Shoc2 at 0 min±s.e. from four experiments is presented on the graph. The relative amount of ubiquitylation in each sample was compared to the Shoc2 ubiquitylation levels in the DMSO-treated cells at 0 min. The *P*-value for DMSO versus P22077 was calculated using a one-tailed paired Student's *t*-test. The results in each panel are representative of three independent experiments. (C) Endogenous Shoc2 was immunoprecipitated from 293FT cells serum-starved for 16 h, treated with vehicle (DMSO) or 25 µM of P22077 for 4 h, and then stimulated with EGF (0.2 ng/ml) for 7 and 15 min. Immunoblots were analyzed with anti-USP7, -RAF-1, -pRAF-1 (Ser338), -pERK1/2, -Shoc2 and GAPDH antibodies. (D) Blots from the multiple experiments were analyzed. Data are mean±s.e. for pRAF-1 normalized to the value for total RAF-1 and compared to pRAF-1 at 0 min (in arbitrary units). The *P*-value for DMSO versus P22077 (7 min) was calculated using a one-tailed paired Student's *t*-test. The results on graph are representative of three independent experiments.

increase in Shoc2-bound RAF-1 phosphorylation observed in control cells (Fig. 4D). The levels of phospho-ERK1/2 were also noticeably higher in control cells compared to P22077-treated cells (Fig. 4C, input). These data indicate that in the Shoc2 scaffolding module, USP7 is likely a part of an inhibitory feedback loop that regulates the amplitude of Shoc2-ERK1/2 signaling (Jang et al., 2019a).

Importantly, the experiments shown in Fig. 4C reveal the unanticipated finding of the strikingly inducible Shoc2-USP7 interaction that reached its maximum 7 min after EGF treatment.

Journal of Cell Science (2021) 134, jcs258922. doi:10.1242/jcs.258922

It was also surprising to find that the peak of Shoc2-bound USP7 was detectable in immunoprecipitates collected before the ubiquitylation of Shoc2 reached its maximum. HUWE1-induced Shoc2 ubiquitylation peaked between 15 to 30 min following EGF treatment (Fig. 4A) (Jang et al., 2019a). Yet, USP7 was found in the Shoc2 complex before the 15 min time point. Interestingly, we also found that inhibition of USP7 by P22077 caused a significant decrease in the levels of USP7 in the Shoc2 immunoprecipitates. Together, these data indicate that the role of USP7 in the Shoc2 module extends beyond the direct de-ubiquitylation of Shoc2 and/or RAF-1 protein.

USP7-Shoc2-HUWE1 complex

USP7 is known for its unique capacity to cooperate and control the activity of several E3 ubiquitin ligases (Kim and Sixma, 2017). Moreover, the E3 ligase HUWE1, similar to other HECT-domain E3 ligases, has been shown to undergo polyubiquitylation (Bernassola et al., 2008). With this notion in mind, we reasoned that in the Shoc2 complex the de-ubiquitylating enzyme USP7 is possibly a part of the HUWE1-mediated feedback loop. Thus, we started by testing whether USP7 modulates ubiquitylation of the Shoc2-bound HUWE1. First, Shoc2 complexes were immunoprecipitated from cells treated with P22077 and stimulated with EGF in the non-denaturing environment (Fig. 5A). Shoc2 immunoprecipitates were then denatured and used to analyze the ubiquitylation of the Shoc2-bound HUWE1 (Fig. 5A). We found that Shoc2 effectively precipitated endogenous E3 ligase HUWE1 and that the Shoc2-HUWE1 interaction was not affected by the activation of the ERK1/2 pathway (Fig. 5A, non-denaturing conditions). Inhibition of USP7 catalytic activity also did not affect Shoc2-HUWE1 binding, supporting the notion that the Shoc2-HUWE1 interaction

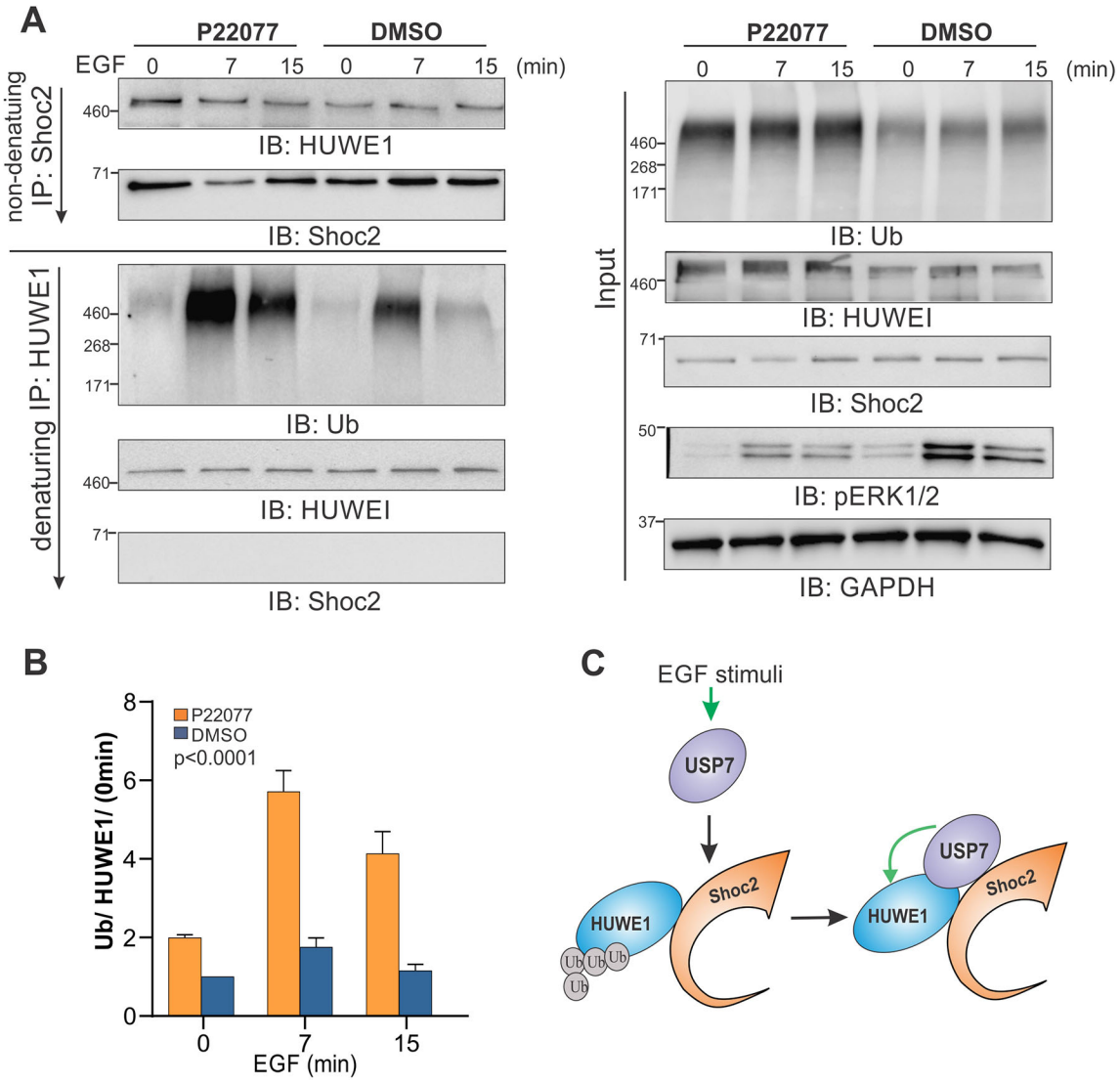

Fig. 5. USP7 regulates ubiquitylation of Shoc2**-bound HUWE1.** (A) The 293FT cells were serum-starved for 16 h, treated with 25 µM of P22077 for 4 h and then stimulated with EGF (0.2 ng/ml) for 7 and 15 min. Endogenous Shoc2 was precipitated under non-denaturing conditions. Half of the immunoprecipitates (IP) were analyzed with anti-Shoc2 and anti-HUWE1 antibodies. The rest of the Shoc2 immunoprecipitates were then denatured and subjected to immunoprecipitation using anti-HUWE1 antibody. HUWE1 ubiquitylation was detected with anti-ubiquitin (Ub) antibody. Immunoblots (IB) were analyzed with anti-Shoc2, HUWE1, -Ub, GAPDH and -pERK1/2 antibodies. (B) Bar graph showing the relative mean amount of Ub normalized to the total amount of HUWE1 and compared to control Ub at 0 min in arbitrary units±s.e. (n=6) [P<0.001 (7 min) was calculated using a two-tailed paired Student's t-test]. The results are representative of six independent experiments. (C) Schematic depicting USP7 removal of HUWE1 ubiquitylation when bound to Shoc2.

Journal of Cell Science (2021) 134, jcs258922. doi:10.1242/jcs.258922

is constitutive (upper panel in Fig. 5A, P22077). We then used denatured Shoc2 immunoprecipitates to analyze HUWE1 ubiquitylation (Fig. 5A, denaturing conditions). Not only was the Shoc2-bound HUWE1 transiently ubiquitylated in response to EGF treatment, but HUWE1 ubiquitylation reached its peak 7 min after EGF stimulation. Importantly, P22077 treatment resulted in a striking increase in the amplitude of ubiquitylation of the Shoc2-bound HUWE1 (Fig. 5B). We also found that USP7 likely modifies ubiquitylation within the HECT domain of HUWE1 (Fig. S5). Critically, an increase in HUWE1 ubiquitylation coincided with attenuated ERK1/2 phosphorylation (Fig. 5A, input). Together, these data suggest that USP7 activity is directed toward the Shoc2-bound HUWE1 (Fig. 5C).

To confirm that USP7 targets the E3 ligase HUWE1 in the Shoc2 complex, we defined the USP7 protein binding site within Shoc2. Computational analysis using the eukaryotic linear motif (ELM) resource (www.elm.eu.org) predicted three USP7 UbL2-binding motifs (probability of 3.742e-03) and one binding motif within the TRAF-like motif of USP7 (probability of 1.239e-02). The predicted TRAF-binding sequence included the pattern [PA][^P][^FYWILA]S[^P] that was within the unstructured N-terminus of Shoc2 (aa28-32, AKASG). All UbL2-3-binding motifs include a KxxxK pattern: KEREK (aa22-26), KVLSK (aa379-383) and KLNMK (aa383-387) (Fig. 6A). The essential lysine amino residues were then mutated to alanines, and the binding of Shoc2 and USP7 was examined either in Shoc2 CRISPR knockout HeLa cells (Fig. 6B) or by using purified recombinant His-tagged Shoc2 and USP7 (Fig. 6C). Although Shoc2$^{K22A/K326A}$ and Shoc2$^{K379A/K383A}$ mutants somewhat retained their ability to bind USP7, the substitutions of K383 and K387 residues for alanine practically abolished the Shoc2-USP7 interaction. These results thus suggest that both binding motifs contribute to the Shoc2-USP7

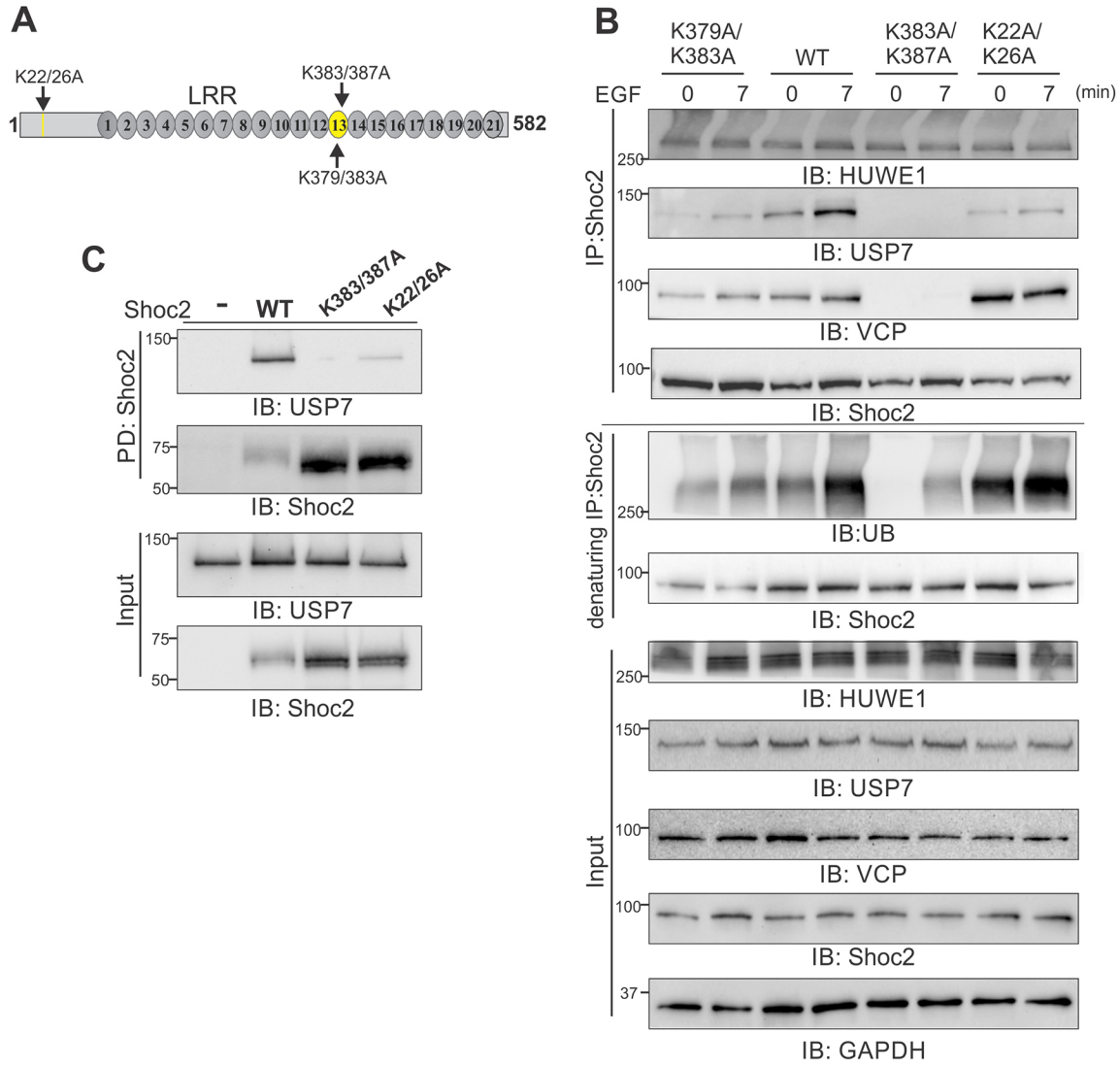

Fig. 6. Dissecting the Shoc2 and USP7 protein interaction. (A) Schematic representation of putative USP7 binding sites within Shoc2. (B) HeLa Shoc2 CRISPR knockout cells were transfected with wild-type (WT) Shoc2-tRFP or mutants. Cells 48 h post transfection were serum-starved for 16 h and then stimulated with EGF (0.2 ng/ml) for 7 min. Shoc2 was precipitated from non-denatured cell lysates and Shoc2 complexes were analyzed with anti-Shoc2, -HUWE1, -USP7 and -VCP antibodies. Shoc2 was also precipitated from denatured cell lysates using anti-Shoc2 antibodies and its ubiquitylation was detected with anti-ubiquitin (Ub) antibody. Cell lysates were analyzed with anti-Shoc2, -HUWE1, -USP7, -VCP and - GAPDH antibodies. The results in each panel are representative of four independent experiments. (C) Recombinant wild-type and mutated His-Shoc2 proteins were mixed with GST-USP7 coupled to glutathione Sepharose beads. Complexes were analyzed using anti-Shoc2 and -USP7 antibodies. The results in each panel are representative of three independent experiments. IB, immunoblot; IP, immunoprecipitated; LRR, leucine-rich repeat.

Journal of Cell Science (2021) 134, jcs258922. doi:10.1242/jcs.258922

interaction. In addition, we found that the ubiquitylation of the Shoc2$^{K383A/K387A}$ mutant was dramatically reduced when the ubiquitylation of the Shoc2$^{K22A/K26A}$ mutant was significantly increased, even though Shoc2-HUWE1 binding was not affected (Fig. 6B). These unexpected findings point toward the possible involvement of additional molecules, and further studies will be required to fully understand the complex molecular underpinnings of these observations. Finally, the loss of ubiquitylation by both the Shoc2$^{K379A/K383A}$ and Shoc2$^{K383A/K387A}$ mutants completely or partially abolished the binding of Shoc2 with valosin-containing protein (VCP), which is in agreement with our earlier findings showing that VCP recognizes only the ubiquitylated species of Shoc2 (Jang et al., 2019a).

When ERK1/2 pathway dynamics were studied in an EGF-dependent time course in cells expressing Shoc2$^{K383A/K387A}$ and Shoc2$^{K22A/K26A}$ mutants, ERK1/2 phosphorylation was dramatically altered at early time points in cells expressing either Shoc2$^{K383A/K387A}$ or Shoc2$^{K22A/K26A}$ mutants compared to wild-type Shoc2. However, little difference was observed between either mutant versus wild-type Shoc2 30 min after EGF treatment (Fig. S6), indicating the effect of the Shoc2-USP7 interaction on a rapid and Shoc2-dependent phase of ERK1/2 activation (Boned Del Rio et al., 2019). These data demonstrate that the loss of USP7 binding modulates Shoc2-guided ERK1/2 phosphorylation.

To investigate the question of whether in the Shoc2 complex USP7 modulates the ubiquitylation of HUWE1 further, we performed sequential immunoprecipitations using HeLa Shoc2 CRISPR knockout cells transiently expressing either wild-type Shoc2 or the Shoc2 mutants $^{K383A/K387A}$ and $^{K22A/K26A}$ (Fig. 7; Fig. S7). First, the Shoc2 complexes were precipitated from the cells stimulated with EGF (0, 7 and 15 min) under non-denaturing conditions (Fig. 7; Fig. S7, non-denaturing IP). The Shoc2 precipitates were then denatured and used to analyze the ubiquitylation of the Shoc2-bound HUWE1 (Fig. 7, denaturing IP). Ubiquitylation of the Shoc2-bound HUWE1 reached its maximum 7 min after EGF treatment. Yet, in the cells expressing the Shoc2$^{K383A/K387A}$ (Fig. 7) or Shoc2$^{K22A/K26A}$ (Fig. S7) mutants, the ubiquitylation levels of the Shoc2-bound HUWE1 were dramatically altered. These data highlight the intricate nature of Shoc2-USP7 binding and further support our hypothesis that in the Shoc2 complex USP7 exerts its activity toward the E3 ligase HUWE1.

To better understand the role of USP7-mediated HUWE1 ubiquitylation, we assessed the ubiquitin chain linkages of USP7-modified HUWE1 using antibodies recognizing either the K48 or K63 chains (Fig. S8). Western blot characterization of the resulting ubiquitin products showed that although the K63-ubiquitylated chains are modified on the HECT domain of HUWE1 they do not change when the activity of USP7 is inhibited (Fig. S8A,B). However, ubiquitin K48 chains are significantly increased in cells treated with the USP7 inhibitor P22077, indicating that the specificity of ubiquitin branching is controlled by USP7.

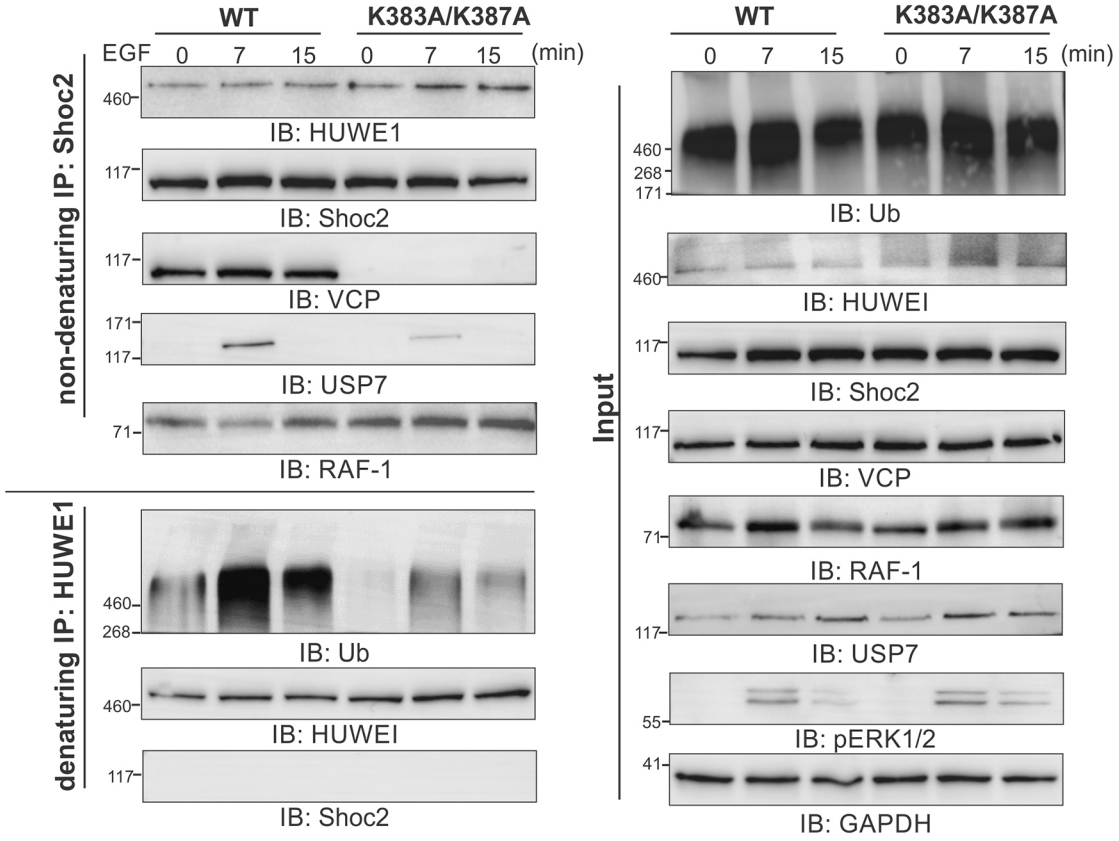

Fig. 7. USP7 regulates ubiquitylation of Shoc2-bound HUWE1. HeLa Shoc2 CRISPR knockout cells expressing wild-type Shoc2-tRFP or the Shoc2 mutant K383/387A were serum starved for 16 h and then stimulated with EGF (0.2 ng/ml) for 7 and 15 min. Endogenous Shoc2 was precipitated under non-denaturing conditions (top left panel). Half of the Shoc2 immunoprecipitates (IP) were analyzed with anti-HUWE1, -VCP, -Shoc2, -USP7 and RAF-1 antibody. The rest of the Shoc2 immunoprecipitates were then denatured and subjected to immunoprecipitation using anti-HUWE1 antibody (bottom left panel). Ubiquitylation was detected with anti-ubiquitin (Ub) antibody. Immunoblots (IB) were analyzed with anti-Shoc2, -Ub and -HUWE1 antibodies. Cell lysates were probed with anti-Ub, -HUWE1, -VCP, -Shoc2, -USP7, pERK1/2, GAPDH and RAF-1 antibody (right panel). The results in each panel are representative of at least three independent experiments. WT, wild type.

Journal of Cell Science (2021) 134, jcs258922. doi:10.1242/jcs.258922

USP7 binding by Shoc2 NSLAH mutations is altered

The data in Fig. 1B,C show that Shoc2 pathogenic variants (Shoc2^{S2G}, Shoc2^{E89D}, Shoc2^{L437I} and Shoc2$^{QH269/270HY}$) are differentially ubiquitylated. Therefore, we examined the binding of the Shoc2 NSLAH-associated variants with USP7. We found that, in contrast to what was observed for wild-type Shoc2 or for the Shoc2 variants for which ubiquitylation was not affected (Shoc2^{C238Y} and Shoc2^{M173I}), the levels of USP7 in the complex with Shoc2^{S2G}, Shoc2^{L437I}, Shoc2$^{QH269/270HY}$ and Shoc2^{E89D} variants remained constant and were not induced by EGF activation (Fig. 8A). Interestingly, all of the Shoc2 pathogenic variants retained their ability to bind HUWE1. The Shoc2^{S2G} and

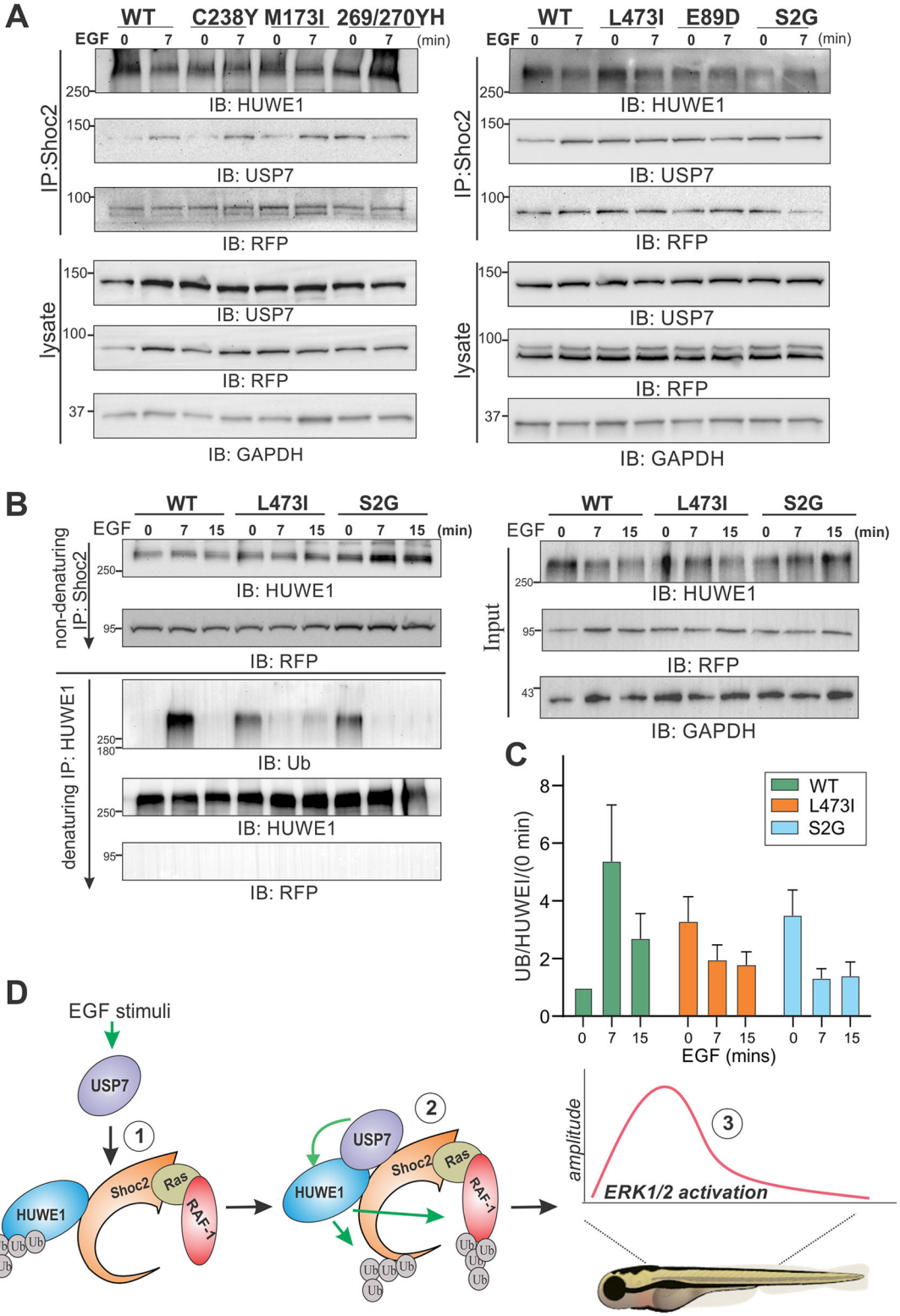

Fig. 8. See next page for legend.

Journal of Cell Science

Journal of Cell Science (2021) 134, jcs258922. doi:10.1242/jcs.258922

Fig. 8. Aberrant USP7 binding and ubiquitylation of Shoc2-bound HUWE1 in cells expressing Shoc2 NSLAH variants. (A) The USP7 binding of the Shoc2 NSLAH variants. HeLa Shoc2 CRISPR knockout cells expressing the Shoc2 variants were serum starved for 16 h and then stimulated with EGF (0.2 ng/ml) for 7 min. Shoc2 was precipitated using anti-Shoc2 antibodies. Immunoblots (IB) were analyzed with anti-Shoc2, -USP7 and -HUWE1 antibodies. The results in each panel are representative of three independent experiments. (B) HeLa Shoc2 CRISPR knockout cells expressing wild-type (WT) Shoc2-tRFP or the Shoc2 S2G or L473I mutants were serum starved for 16 h and then stimulated with EGF (0.2 ng/ml) for 7 and 15 min. Shoc2 complexes were precipitated under non-denaturing conditions (top left panel) using anti-Shoc2 antibody. Half of the of Shoc2 immunoprecipitates (IP) were analyzed with anti-HUWE1 and -RFP antibody. The rest of the Shoc2 immunoprecipitates were then denatured and subjected to immunoprecipitation using anti-HUWE1 antibody (bottom left panel). Ubiquitylation was detected with anti-ubiquitin (Ub) antibody. Immunoblots were analyzed with anti-RFP, -Ub and -HUWE1 antibodies. Cell lysates were probed with anti-HUWE1, -RFP and -GAPDH antibodies. The results in each panel are representative of at least four independent experiments. (C) Bar graph showing the relative mean amount of Ub normalized to the total amount of HUWE1 and compared to control Ub at 0 min in arbitrary units±s.e. (n=6). (D) Schematic showing the working model depicting what is currently understood for the mechanisms by which USP7 modulates the Shoc2-mediated ERK1/2 signals. Activation of the ERK1/2 pathway is followed by recruitment of USP7 to the Shoc2-HUWE1 complex. In the Shoc2 complex, USP7 exerts it activity toward HUWE1 and potentiates ubiquitylation of Shoc2 and RAF-1, leading to the adjustments in the amplitude of ERK1/2 signaling. Disruption in the molecular mechanisms regulating the amplitude of ERK1/2 signals results in abnormal embryonic development.

Shoc2^{L437I} variants were thus used to examine whether the ubiquitylation of Shoc2-bound HUWE1 was also altered. We again performed sequential immunoprecipitations of HUWE1 from HeLa Shoc2 CRISPR knockout cells transiently expressing either wild-type Shoc2 or the Shoc2^{S2G} and Shoc2^{L437I} mutants (Fig. 8B). First, the Shoc2 complexes were precipitated from cells stimulated with EGF (0, 7 and 15 min) under non-denaturing conditions. The Shoc2 precipitates were then denatured and used to analyze the ubiquitylation of the Shoc2-bound HUWE1 (Fig. 8B, denaturing). In cells expressing wild-type Shoc2, ubiquitylation of the Shoc2-bound HUWE1 reached its maximum 7 min after EGF treatment. Yet, in the cells expressing the Shoc2^{S2G} or Shoc2^{L437I} mutants, the ubiquitylation levels of the Shoc2-bound HUWE1 were significantly decreased. Moreover, the dynamics of the ubiquitylation of HUWE1 bound to the Shoc2^{L437I} and Shoc2$^{QH269/270HY}$ variants were altered with its maximum prior to ERK1/2 pathway activation (Fig. 8C). These data lend additional support to the notion that in the Shoc2 complex USP7 exerts its activity toward the E3 ligase HUWE1 and suggest that USP7 likely removes inhibitory ubiquitylation from the HECT domain. Although, molecular details of this activity are not clear and require additional studies. Most importantly, together with our *in vivo* studies, these experiments provide strong support for the hypothesis that dysregulated USP7-Shoc2 interaction and Shoc2 ubiquitylation are the factors contributing to NSLAH pathogenesis.

DISCUSSION

The results presented here highlight a critical role for the de-ubiquitylating enzyme USP7 in the pathogenesis of NSLAH syndrome, and illustrate an unexpected complexity of the mechanisms regulating the Shoc2-ERK1/2 signaling axis. These findings show that USP7 is an integral partner within the Shoc2 signaling module and explain the role of USP7 in the Shoc2 module. Importantly, they establish that in the Shoc2 complex USP7 has dual activity: (1) to modulate ubiquitin levels on the E3 ligase HUWE1, possibly through preventing its auto-ubiquitylation; and (2) to control ubiquitylation of Shoc2 through the de-ubiquitylation of HUWE1, thereby allowing for a rapid regulatory feedback loop in which the amplitude of the ERK1/2 signals is rapidly modulated.

The role of USP7 in the Shoc2 complex

The de-ubiquitylating enzyme USP7 is a highly abundant protein, with many interacting partners, that is implicated in numerous cellular processes, such as DNA repair, endosomal protein trafficking, chromatin dynamics, metabolism and cell survival, proliferation or apoptosis (Hao et al., 2015; Jagannathan et al., 2014; Khoronenkova et al., 2012; Liefke et al., 2017; Pozhidaeva and Bezsonova, 2019). USP7 stabilizes many of its targets (e.g. E3 ligase MDM2, p53, Foxos, ANAX1, etc) (Epping et al., 2011; Hall et al., 2014; Hao et al., 2015; Saridakis et al., 2005; Sheng et al., 2006; van der Horst et al., 2006; Wang et al., 2019). It has been shown that USP7 also can form stable protein complexes with several other interacting partners that serve as scaffolds (Ye et al., 2015). These partners localize USP7 to the correct place (Hao et al., 2015) and/or modulate its activity (Faesen et al., 2011; van der Knaap et al., 2005). Our study provides compelling evidence that USP7 interacts with Shoc2 in cells and *in vitro*, and in the absence of other components of the Shoc2 complex. Here, we show that USP7 function goes beyond stabilizing levels of Shoc2 or its known partners RAF-1 and HUWE1 (Fig. 3; Figs S3, S4). We also find that Shoc2 and USP7 interact in a bipartite manner, with Shoc2 recognizing both the N-terminal TRAF/MATH domain, as well as the C-terminal UbL region of USP7 (Fig. S2).

The finding that USP7 binds to Shoc2 in a transient EGF-dependent manner (Fig. 4) is one of the most intriguing observations of this study. These data unravel a novel mode of action for USP7 in the Shoc2 complex and indicate that USP7 de-ubiquitylation may regulate the activity of the E3 ligase HUWE1 in the Shoc2 complex. Moreover, the experiments in Figs 5–7 demonstrate that HUWE1 is the primary target of USP7, as abrogated binding of Shoc2 and USP7, or a decrease in the enzymatic activity of USP7, alters the levels of ubiquitin modified on Shoc2-bound HUWE1. These data are consistent with earlier evidence pointing to an unusual propensity of USP7 to protect different E3 ligases (e.g. MDM2, UHRF1, TRIM27, etc) from auto-ubiquitylation, thus allowing for their maximal E3 ligase activity (Kim and Sixma, 2017).

We also show that failure to recruit USP7 by Shoc2 leads to changes in the ubiquitin levels of HUWE1 coinciding with aberrations in the rapid phosphorylation of Shoc2-bound RAF-1 and ERK1/2 (Fig. 4). Collectively, these data establish that Shoc2 incorporates the de-ubiquitylase USP7 to provide an additional layer of control over the amplitude of the ERK1/2 signals transmitted through the module. Our biochemical experiments lead to an updated model of how negative feedback mechanisms control the amplitude of signals transmitted via the Shoc2-ERK1/2 signaling axis (Fig. 8D). In this model, EGF-dependent activation of the ERK1/2 pathway induces binding of USP7 to the Shoc2 complex (step 1), in which USP7 controls the ability of HUWE1 to modify the noncatalytic scaffold Shoc2 (step 2). HUWE1-mediated ubiquitylation of Shoc2 and RAF-1 allows for the dynamic range of RAF-1 activity to be fine-tuned, thereby actively monitoring the transmission of ERK1/2 signals (step 3). Future studies will resolve remaining questions regarding the molecular events triggering the recruitment of USP7 to the Shoc2 complex, and will determine

Journal of Cell Science (2021) 134, jcs258922. doi:10.1242/jcs.258922

whether in the Shoc2 complex USP7 shows similar levels of cooperativity to what was previously observed for USP7 in the MAGE-L2-TRIM27 complex or other USP7-E3 ligase pairs (Hao et al., 2015).

Mechanisms underlying a USP7-HUWE1-Shoc2 regulatory loop

The bipartite Shoc2-USP7 recognition raises an obvious question as to what structural features are recognized via this bipartite binding and what is the significance of such a recognition pattern. In the case of USP7 partners GMP-synthetase (GMPS) and DNMT1 (Cheng et al., 2015; Faesen et al., 2011; Kim et al., 2016), similar recognition allows GMPS and UVSSA to allosterically regulate and stabilize the active state of the TRAF/MATH domain of USP7 by promoting the interaction of the TRAF domain with UBL4/5, which is needed for the full activation of USP7 (Kim et al., 2016; Sarasin, 2012; Schwertman et al., 2012, 2013). Thus, taking into account the scaffolding properties of Shoc2, it is conceivable that Shoc2-USP7 bipartite recognition is a possible mechanism by which Shoc2 modulates the interaction between the catalytic and the UbL domains of USP7, thereby either promoting the 'on' state, like GMP synthetase (Faesen et al., 2011) or sequestering UbL domains from the catalytic domain and promoting the 'off' state.

It is also tempting to speculate that ubiquitin moieties removed from the HECT domain of HUWE1 by USP7 (Fig. S5; Pandya et al., 2010) are de-activating auto-ubiquitylation. In this scenario, dissociation of USP7 from Shoc2 will then lead to Shoc2 de-ubiquitylation, possibly eliciting a conformational change in the scaffold itself, thereby reducing its ability to facilitate USP7 activation. HUWE1-mediated feedback regulating USP7 is also plausible in this scenario. Future studies exploring the molecular basis of the direct interaction between USP7, HUWE1 and Shoc2 will resolve these intriguing possibilities and provide important mechanistic details on active remodeling within the scaffolding module.

Our data suggest that upon EGF treatment HUWE1 does not dissociate from the Shoc2 complex as no apparent change in the levels of the Shoc2-bound HUWE1 was detected. Yet, if HUWE1 remains bound to Shoc2 then our observations of UPS7 removing K48 ubiquitin chains from the HECT domain of HUWE1 are rather puzzling (Fig. S8). Additional analysis will be necessary to establish the role of the K48 ubiquitin linkages.

Importantly, this study provides new evidence that ubiquitin modifications within the Shoc2 scaffold complex play a critical and active role in controlling Shoc2-transmitted ERK1/2 signals. The transient nature of the USP7-Shoc2 interaction and its potential ability to modulate – increase/decrease the catalytic efficiency of HUWE1 – provides the means for a rapid and effective response to external stimuli. Dynamic changes within Shoc2 ubiquitylation and USP7 binding also indicate that another de-ubiquitylating enzyme possibly assists in the 'reactivation' of the Shoc2 module.

Implications for NSLAH pathology

In addition to identifying a role for USP7 in the transmission of ERK1/2 signals, we also report the involvement of USP7 in the mechanisms underlying NSLAH pathology (Figs 1, 2 and 8). Our analysis of searchable databases revealed several patients harboring novel Shoc2 variants and presenting with several developmental and behavioral phenotypes overlapping with NSLAH (e.g. congenital heart defects, developmental delay/intellectual disability, distinctive craniofacial dysmorphisms, short stature, feeding difficulties and fine hair) (Cordeddu et al., 2009; Hannig et al., 2014; Motta et al., 2019; Tidyman and Rauen, 2016). Although we cannot exclude that some of the phenotypes observed in these patients may be attributed to a mutation in other associated genes (Table S1), our zebrafish experiments firmly support the pathogenicity of the L473I variant. Even though the Shoc2 variants analyzed in this study are not within the identified USP7-binding domains of Shoc2, increased ubiquitylation of the S2G, QH269/270HY and L473I pathogenic variants, and the aberrant recognition of USP7, indicate that disruptions in the USP7-initiated feedback loop of the Shoc2-ERK1/2 axis contribute to the Shoc2-associated NSLAH pathology. Other proteins likely facilitate the recognition of Shoc2 and USP7, and the defects in the dynamics of USP7-Shoc2 binding observed in the S2G, QH and L473I variants are due to the disrupted USP7-adapter-Shoc2 recognition. Additional studies providing a plausible mechanism for the observed tissue-specific developmental defects of all novel Shoc2 gene variants are needed to clarify how the disease-associated genetic variants alter the function of Shoc2. These studies will improve our understanding of the consequences that Shoc2 variants have on development, as well as the pathogenesis of the disease.

DUBs have been shown to control different aspects of embryonic development (Basar et al., 2021) and are commonly found to regulate stem cell maintenance and differentiation by controlling gene expression (Gu et al., 2019; Pei, 2017). Some DUBs have been shown to modulate fundamental signaling pathways (e.g. FGF, WNT and Notch) (Clague et al., 2012; Jin et al., 2016; Ma et al., 2014; Novellasdemunt et al., 2017). Disruption of one allele of USP7 results in Hao-Foutain syndrome, a developmental disorder with seizures, behavioral abnormalities and hypotonia (Hao et al., 2015). The role of USP7 in the regulation of neuronal differentiation is attributed to its function in the regulation of retromer-dependent endosomal recycling of membrane proteins (Hao et al., 2015). It is also noteworthy that USP7 has been identified as one of the 57 DUB genes that are required for the early development of zebrafish (Tse et al., 2009). Similar to the loss of Shoc2, the loss of USP7 resulted in profound defects in craniofacial cartilages (Jang et al., 2019b). Thus, it will be interesting to determine whether the Shoc2 mutations affecting Shoc2-USP7 binding cause abnormalities similar to the USP7-caused Hao-Fountain syndrome. Likewise, further studies are needed to clarify the pathophysiological significance of the interaction between Shoc2 and USP7 for the pathogenesis of Hao-Fountain syndrome.

In summary, these studies are the first to identify USP7 as a part of the ERK1/2 canonical signaling pathway and to provide insights into a new mechanism modulating activation of this cascade. Ours is also the first report suggesting that this role in controlling post-translational modification is evolutionarily conserved. Here, we provide new insights into the signaling mechanisms and emphasize how vital it is to understand the molecular and cellular basis of diseases for dissecting disease pathogenesis. The Shoc2 scaffold is a complex module that regulates various cellular functions (Jang et al., 2021). Thus, it is reasonable to assume that deregulation of the mechanisms that control the function of the Shoc2 assembly will have pathological consequences. Future studies of Shoc2 complexes will resolve the remaining questions and identify additional proteins regulating the dynamics within the scaffold complex, as well as the full extent of the mechanisms by which signals transmitted through the complex are regulated. Knowing the precise etiology and pathogenesis of Shoc2-related malformations is also essential for the development of therapeutic avenues for the minimization or prevention of various anomalies in other RASopathies.

Journal of Cell Science (2021) 134, jcs258922. doi:10.1242/jcs.258922

MATERIALS AND METHODS

Antibodies and other reagents

Specific proteins were detected using primary antibodies against the following: M-RAS, RAF-1, GST, GFP, HA, phosphorylated ERK1/2 (pERK1/2), ubiquitin, cyclin D1 and GAPDH (Santa Cruz Biotechnology, Dallas, TX, USA); Shoc2, USP7 and HUWE1 (Proteintech, Rosemont, IL, USA); phosphorylated RAF-1 [pRAF-1 (S338)], K-48 or K-63 link ubiquitin (Cell Signaling Technology, Danvers, MA, USA); VCP (BioLegend, San Diego, CA, USA); tag red fluorescent protein (Thermo Fisher Scientific); humanized synthetic sdAbs 99 (hs2dAbs99) against Shoc2 (previous developed and characterized by Jang et al., 2020); and peroxidase-conjugated AffiniPure F(ab′)2 fragment goat anti-rabbit IgG and Mouse IgG (H+L) (Jackson ImmunoResearch). Purified USP7 protein was purchased from Sino Biological. EGF was purchased from BD Biosciences, HBX 41108 from Tocris Bioscience, P22077 from Selleckchem (Houston, TX, USA), cycloheximide and MG132 from Enzo, and *N*-ethylmaleimide (NEM) was obtained from Thermo Scientific/Pierce.

Cell culture and DNA transfections

Cos1cells [American Type Culture Collection (ATCC)], 293FT cells (Invitrogen), HeLa cells (ATCC) and stable cell lines (derivatives of HeLa cells) were grown in Dulbecco modified Eagle's medium (DMEM) containing 10% fetal bovine serum (FBS) supplemented with sodium pyruvate, minimal essential medium with nonessential amino acids (MEM-NEAA), penicillin, streptomycin and L-glutamate (Invitrogen). Transfections of DNA constructs were performed using polyethyleneimine (Neo Transduction Laboratories, Lexington, KY, USA) or TransIT-HeLaMonster (MirusBio LLC) reagent. Expression of proteins was confirmed by western blotting, as described below.

Expression plasmids

tRFP-tagged Shoc2 (Shoc2-tRFP) has been described previously (Jeoung et al., 2013). Shoc2-tRFP-tagged mutants were generated as described previously (Jeoung et al., 2013). A mammalian GST expression vector was kindly provided by Haining Zhu (University of Kentucky, Lexington, KY, USA). A His-tag protein expression vector for Shoc2 purification was kindly provided by Craig Vander Kooi (University of Kentucky, Lexington, KY, USA). USP7 constructs were kindly provided by Dr Ryan Potts (St. Jude Children's Hospital, Memphis, TN, USA). All constructs were verified by dideoxynucleotide sequencing.

siRNA transfections

To silence protein expression by RNAi, cells were seeded in 12-well plates (at 50 to 60% confluence with 1 ml of DMEM-FBS per well) at least 20 h before transfection. siRNA transfections were performed at 24- to 36-h intervals according to the manufacturer's recommendations, using Dharmafect reagent 2 (Thermo Fisher Scientific/Dharmacon). The siRNA sequence used to target HUWE1 transcripts was as follows: 5′-GAGU-UUGGAGUUUGUGAAGTT-3′ (Jang et al., 2014). The siRNA sequence used to target the USP7 transcripts was as follows: 5′-GUAAAGAAGUA-GACUAUCG-3 (Thompson et al., 2014). The efficiency of the siRNA knockdown was validated by western blotting.

CRISPR/Cas9-mediated gene deletion

A HeLa cell line lacking Shoc2 was generated by Biocytogen (www.biocytogen.com). RNA guide sequences (5′-GATAAAGGTATTGCCTC-TGT TGG3-′ and 5′-GGAATAAAGGTCAAAAGATT AGG-3′) targeting exon 2 and CRISPR/Cas9 technology was used to insert a puromycin resistance gene. Clones were isolated, screened genetically and then tested for Shoc2 expression by immunoblot. Gene disruption was also validated by PCR analysis.

Immunoprecipitation and western blot analysis

Cells were placed on ice and washed with Ca^{2+}, Mg^{2+}-free PBS, and the proteins were solubilized in 50 mM Tris (pH 7.5) containing 150 mM NaCl, 1% Triton X-100, 1 mM Na_3VO_4, 10 mM NaF, 0.5 mM phenylmethylsulfonyl fluoride (Sigma-Aldrich, St. Louis, MO, USA), 10 µg/ml leupeptin, and 10 µg/ml aprotinin (Roche, Basel, Switzerland) for 15 min at 4°C. Lysates were then centrifuged at 16,000 ***g*** for 15 min to remove insoluble material. Lysates were incubated with appropriate antibodies for 2 h, and the immunocomplexes were precipitated using protein A- or G-Sepharose (GE Healthcare Life Sciences, Chicago, IL, USA). Immunoprecipitates and aliquots of cell lysates were denatured in sample buffer at 95°C, resolved by electrophoresis and probed by western blotting with various antibodies followed by chemiluminescence detection.

Western blotting was performed as described previously (Jeoung et al., 2013). Proteins transferred from SDS-polyacrylamide gels to nitrocellulose membranes were visualized using a ChemiDoc analysis system (Bio-Rad, Hercules, CA, USA). Several exposures were analyzed to determine the linear range of the chemiluminescence signals. Quantification was performed using the densitometry analysis mode of Image Lab software (Bio-Rad).

Denaturing immunoprecipitation for *in vivo* ubiquitylation assay

Denaturing immunoprecipitation was performed as described previously (Jang et al., 2015). Briefly, cells were lysed in denaturing buffer [50 mM Tris (pH 7.5), 150 mM NaCl, 1% Triton X-100, 1% SDS, 1 mM Na_3VO_4, 10 mM NaF, 5 mM NEM and 10 µM MG132] and boiled for 10 min. Lysates were diluted 1:10 with the same buffer without SDS and incubated with the appropriate antibody overnight with rotation at 4°C. Protein G-agarose (GE Healthcare Life Sciences, Chicago, IL, USA) was added and the agarose beads were washed four times in lysis buffer (without SDS). Proteins were eluted at 95°C in SDS loading buffer, separated by SDS-PAGE and transferred to a nitrocellulose membrane.

Interaction of recombinant proteins

GST- and His-tagged proteins were affinity purified from bacterial cells using standard protocols as described by Jang et al. (2020). Briefly, GST and GST-USP7 (full-length or truncated mutants) were produced in BL21(DE3) cells by overnight induction at 16°C with 0.5 mM isopropyl b-D-1-thiogalactopyranoside (IPTG). Proteins were purified from bacterial lysates with glutathione sepharose (GE Amersham) and eluted with 10 mM glutathione. Proteins were stored in PBS containing 10% glycerol. *In vitro* binding assays were performed as described by Jang et al. (2020). Briefly, 1.5 µg of purified GST-tagged proteins were bound to glutathione Sepharose beads (Goldbio) for 1 h in binding buffer. Equal amounts of full-length USP7 or truncated mutants coupled to glutathione Sepharose beads were then incubated with recombinant His-Shoc2 at 4°C for 16 h. The beads were washed four times with cell lysis buffer and eluted with 2× Laemmli sample buffer.

Zebrafish strains and maintenance

All zebrafish strains were bred, raised and maintained in accordance with established animal care protocols for zebrafish husbandry. Embryos were staged as described previously (Kimmel et al., 1995). All animal procedures were carried out in accordance with guidelines established by the University of Kentucky Institutional Animal Care and Use Committee.

Morpholino and mRNA injection

All MOs were obtained from Gene Tools (Philomath, OR, USA) and injected into one- or two-cell-stage zebrafish embryos. The following MOs were used in this study: standard control MO, 5′-CCTCTTACCTCAGTTACAATT-TATA-3′, and *shoc2* MO: 5′-TACTGCTCATGGCGAAAGCCCCGCA-3′. Embryos were injected with 8 ng each of MOs. For mRNA rescue experiments, the zebrafish *shoc2* coding sequences (with silent mutation at MO target sites) for either wild type or mutant were PCR amplified from zebrafish *shoc2* cDNA and cloned into the pCS2+ vector (Promega, WI, USA). The capped mRNAs were synthesized using the mMessage mMACHINE SP6 transcription kit (Thermo Fisher Scientific, CA, USA) according to the manufacturer's instructions. For mRNA rescue experiments, 100 pg/embryo of wild type was co-injected with 8 ng of *shoc2* MO.

Staining methods and evaluation

Whole-embryo staining for erythropoietic cells was performed using *o*-Dianisidine histochemistry according to previously described methods

(Detrich et al., 1995; Iuchi and Yamamoto, 1983). PTU (1-phenyl-2-thioure)-treated dechorionated embryos were stained for 50 min in the dark in *o*-Dianisidine (0.6 mg/ml), 0.01 M sodium acetate, 0.65% H_20_2, and 40% (v/v) ethanol. After staining, embryos were washed with PBS with 0.1% Tween-20 (PBS-T) and then postfixed in 4% paraformaldehyde overnight in 4°C. Stained embryos were then washed with PBS-T and stored in 90% glycerol for imaging.

To evaluate mRNA rescue, test MOs were injected either singly or in combination with a verified mRNA. Resulting embryos were scored for intensity of *o*-Dianisidine at 52 h post fertilization based on the three classes described previously (Jang et al., 2019b). The evaluators (E.G. and R.N.) were blinded to the identity of the injected embryos at the time of survey. Percentages reflect the total embryos in each staining class summed over three separate experiments. Differences in phenotypical changes were compared using χ^2 tests.

Photography and image analysis

Images of *o*-Dianisidine staining were imaged with Leica DFC7000T mounted on a dissecting microscope (Leica M165 FC, Germany) or with a Leica DFC450 digital camera, and mounted on a dissecting microscope (Leica S9D, Germany). LASX V2.6 software (Leica, Germany) was used to calculate the positive signals. All images were compiled in Adobe Photoshop CS6 Portable (Adobe Systems Incorporated, CA, USA) and resized.

Human subjects

The publicly available DECIPHER database was queried in February 2020. The DECIPHER database contained ∼54,861 individuals at the time of query. We limited our search to those deletions smaller than 5 mb in size and to single nucleotide variants. For subjects in the DECIPHER database, patient consent was obtained by the attending geneticist for public and collaborative group data sharing, giving access to genomic and phenotypic data, and patient reports. Following database use, the providers were contacted to fill out a questionnaire.

Statistical analyses

Results are expressed as mean±s.e.m. The statistical significance of the differences between groups were determined using either paired with one- or two-tailed Student's *t*-tests or one-way ANOVA (followed by the Tukey's test, or Kruskal–Wallis test), as indicated in the legends. $P<0.05$ was considered statistically significant. Phenotypical differences were evaluated using a χ^2 test. All statistical analyses were carried out using GraphPad Prism 8.0 (GraphPad Prism Software Inc., Chicago, IL, USA).

Acknowledgements

We thank Drs Tianyan Gao, Louis Hersh, Ann Morris and Charles Waechter for critical reading of the manuscript, and Ryan Potts for providing critical reagents. This study makes use of data generated by the DECIPHER community who bear no responsibility for the further analysis or interpretation of the data. A full list of centers who contributed to the generation of the data is available from www.decipher.sanger.ac.uk/about/stats and via email from decipher@sanger.ac.uk. Funding for the DECIPHER project was provided by The Wellcome Trust. Some of the text in this paper formed part of Hyeln Jang's PhD thesis in the Department of Molecular and Cellular Biochemistry at the University of Kentucky in 2018.

Competing interests

The authors declare no competing or financial interests.

Author contributions

Conceptualization: E.G.; Methodology: P.W.; Software: R.N.; Investigation: P.W., L.A., E.R.J.; Resources: M.P.; Writing - original draft: E.G.; Visualization: L.A., R.N.; Supervision: E.G.; Project administration: E.G.; Funding acquisition: E.G.

Funding

This project was supported by grants from the National Institute of General Medical Sciences, National Institutes of Health and the Office of Extramural Research, National Institutes of Health (R35GM136295 and 1S10OD025033-01, respectively, to E.G.). Its contents are solely the responsibility of the authors and do not necessarily represent the official views of the National Institute of Health. Deposited in PMC for release after 12 months.

Peer review history

The peer review history is available online at https://journals.biologists.com/jcs/article-lookup/doi/10.1242/jcs.258922.

References

Baldassarre, G., Mussa, A., Banaudi, E., Rossi, C., Tartaglia, M., Silengo, M. and Ferrero, G. B. (2014). Phenotypic variability associated with the invariant Shoc2 c.4A>G (p.Ser2Gly) missense mutation. *Am. J. Med. Genet. A* **164**, 3120-3125. doi:10.1002/ajmg.a.36697

Basar, M. A., Beck, D. B. and Werner, A. (2021). Deubiquitylases in developmental ubiquitin signaling and congenital diseases. *Cell Death Differ.* **28**, 538-556. doi:10.1038/s41418-020-00697-5

Bernassola, F., Karin, M., Ciechanover, A. and Melino, G. (2008). The HECT family of E3 ubiquitin ligases: multiple players in cancer development. *Cancer Cell* **14**, 10-21. doi:10.1016/j.ccr.2008.06.001

Besche, H. C., Haas, W., Gygi, S. P. and Goldberg, A. L. (2009). Isolation of mammalian 26S proteasomes and p97/VCP complexes using the ubiquitin-like domain from HHR23B reveals novel proteasome-associated proteins. *Biochemistry* **48**, 2538-2549. doi:10.1021/bi802198q

Boned del Rio, I., Young, L. C., Sari, S., Jones, G. G., Ringham-Terry, B., Hartig, N., Rejnowicz, E., Lei, W., Bhamra, A., Surinova, S. et al. (2019). Shoc2 complex-driven RAF dimerization selectively contributes to ERK pathway dynamics. *Proc. Natl. Acad. Sci. USA* **116**, 13330-13339. doi:10.1073/pnas.1902658116

Cheng, J., Yang, H., Fang, J., Ma, L., Gong, R., Wang, P., Li, Z. and Xu, Y. (2015). Molecular mechanism for USP7-mediated DNMT1 stabilization by acetylation. *Nat. Commun.* **6**, 7023. doi:10.1038/ncomms8023

Choi, J.-H., Oh, M.-Y., Yum, M.-S., Lee, B. H., Kim, G.-H. and Yoo, H.-W. (2015). Moyamoya syndrome in a patient with noonan-like syndrome with loose anagen hair. *Pediatr. Neurol.* **52**, 352-355. doi:10.1016/j.pediatrneurol.2014.11.017

Clague, M. J., Coulson, J. M. and Urbé, S. (2012). Cellular functions of the DUBs. *J. Cell Sci.* **125**, 277-286. doi:10.1242/jcs.090985

Cordeddu, V., Di Schiavi, E., Pennacchio, L. A., Ma'ayan, A., Sarkozy, A., Fodale, V., Cecchetti, S., Cardinale, A., Martin, J., Schackwitz, W. et al. (2009). Mutation of Shoc2 promotes aberrant protein N-myristoylation and causes Noonan-like syndrome with loose anagen hair. *Nat. Genet.* **41**, 1022-1026. doi:10.1038/ng.425

Couser, N. L., Keelean-Fuller, D., Davenport, M. L., Haverfield, E., Masood, M. M., Henin, M. and Aylsworth, A. S. (2018). Cleft palate and hypopituitarism in a patient with Noonan-like syndrome with loose anagen hair-1. *Am. J. Med. Genet. A* **176**, 2024-2027. doi:10.1002/ajmg.a.40432

Detrich, H. W., III, Kieran, M. W., Chan, F. Y., Barone, L. M., Yee, K., Rundstadler, J. A., Pratt, S., Ransom, D. and Zon, L. I. (1995). Intraembryonic hematopoietic cell migration during vertebrate development. *Proc. Natl. Acad. Sci. USA* **92**, 10713-10717. doi:10.1073/pnas.92.23.10713

Epping, M. T., Meijer, L. A. T., Krijgsman, O., Bos, J. L., Pandolfi, P. P. and Bernards, R. (2011). TSPYL5 suppresses p53 levels and function by physical interaction with USP7. *Nat. Cell Biol.* **13**, 102-108. doi:10.1038/ncb2142

Faesen, A. C., Dirac, A. M. G., Shanmugham, A., Ovaa, H., Perrakis, A. and Sixma, T. K. (2011). Mechanism of USP7/HAUSP activation by its C-terminal ubiquitin-like domain and allosteric regulation by GMP-synthetase. *Mol. Cell* **44**, 147-159. doi:10.1016/j.molcel.2011.06.034

Firth, H. V., Richards, S. M., Bevan, A. P., Clayton, S., Corpas, M., Rajan, D., Van Vooren, S., Moreau, Y., Pettett, R. M. and Carter, N. P. (2009). DECIPHER: database of chromosomal imbalance and phenotype in humans using ensembl resources. *Am. J. Hum. Genet.* **84**, 524-533. doi:10.1016/j.ajhg.2009.03.010

Gargano, G., Guidotti, I., Balestri, E., Vagnarelli, F., Rosato, S., Comitini, G., Wischmeijer, A., La Sala, G. B., Iughetti, L., Cordeddu, V. et al. (2014). Hydrops fetalis in a preterm newborn heterozygous for the c.4A>G Shoc2 mutation. *Am. J. Med. Genet. A* **164**, 1015-1020. doi:10.1002/ajmg.a.36376

Gu, H., Shi, X., Liu, C., Wang, C., Sui, N., Zhao, Y., Gong, J., Wang, F., Zhang, H., Li, W. et al. (2019). USP8 maintains embryonic stem cell stemness via deubiquitination of EPG5. *Nat. Commun.* **10**, 1465. doi:10.1038/s41467-019-09430-4

Hall, J. A., Tabata, M., Rodgers, J. T. and Puigserver, P. (2014). USP7 attenuates hepatic gluconeogenesis through modulation of FoxO1 gene promoter occupancy. *Mol. Endocrinol.* **28**, 912-924. doi:10.1210/me.2013-1420

Hannig, V., Jeoung, M., Jang, E. R., Phillips, J. A., III and Galperin, E. (2014). A novel Shoc2 variant in rasopathy. *Hum. Mutat.* **35**, 1290-1294. doi:10.1002/humu.22634

Hao, Y.-H., Fountain, M. D., Jr., Fon Tacer, K., Xia, F., Bi, W., Kang, S.-H. L., Patel, A., Rosenfeld, J. A., Le Caignec, C., Isidor, B. et al. (2015). USP7 acts as a molecular rheostat to promote WASH-dependent endosomal protein recycling and is mutated in a human neurodevelopmental disorder. *Mol. Cell* **59**, 956-969. doi:10.1016/j.molcel.2015.07.033

Iuchi, I. and Yamamoto, M. (1983). Erythropoiesis in the developing rainbow trout, Salmo gairdneri irideus: histochemical and immunochemical detection of erythropoietic organs. *J. Exp. Zool.* **226**, 409-417. doi:10.1002/jez.1402260311
Jagannathan, M., Nguyen, T., Gallo, D., Luthra, N., Brown, G. W., Saridakis, V. and Frappier, L. (2014). A role for USP7 in DNA replication. *Mol. Cell Biol.* **34**, 132-145. doi:10.1128/MCB.00639-13
Jang, E. R. and Galperin, E. (2016). The function of Shoc2: a scaffold and beyond. *Commun. Integr. Biol.* **9**, e1188241. doi:10.1080/19420889.2016.1188241
Jang, E. R., Shi, P., Bryant, J., Chen, J., Dukhante, V., Gentry, M. S., Jang, H., Jeoung, M. and Galperin, E. (2014). HUWE1 is a molecular link controlling RAF-1 activity supported by the Shoc2 scaffold. *Mol. Cell. Biol.* **34**, 3579-3593. doi:10.1128/MCB.00811-14
Jang, E. R., Jang, H., Shi, P., Popa, G., Jeoung, M. and Galperin, E. (2015). Spatial control of Shoc2-scaffold-mediated ERK1/2 signaling requires remodeling activity of the ATPase PSMC5. *J. Cell Sci.* **128**, 4428-4441. doi:10.1242/jcs.177543
Jang, H., Jang, E. R., Wilson, P. G., Anderson, D. and Galperin, E. (2019a). VCP/p97 controls signals of the ERK1/2 pathway transmitted via the Shoc2 scaffolding complex: novel insights into IBMPFD pathology. *Mol. Biol. Cell* **30**, 1655-1663. doi:10.1091/mbc.E19-03-0144
Jang, H., Oakley, E., Forbes-Osborne, M., Kesler, M. V., Norcross, R., Morris, A. C. and Galperin, E. (2019b). Hematopoietic and neural crest defects in zebrafish shoc2 mutants: a novel vertebrate model for Noonan-like syndrome. *Hum. Mol. Genet.* **28**, 501-514. doi:10.1093/hmg/ddy366
Jang, H., Wilson, P. G., Sau, M., Chawla, U., Rodgers, D. W. and Galperin, E. (2020). Single-domain antibodies for functional targeting of the signaling scaffold Shoc2. *Mol. Immunol.* **118**, 110-116. doi:10.1016/j.molimm.2019.12.010
Jang, H., Stevens, P., Gao, T. and Galperin, E. (2021). The leucine-rich repeat signaling scaffolds Shoc2 and Erbin: cellular mechanism and role in disease. *FEBS J.* **288**, 721-739. doi:10.1111/febs.15450
Jeoung, M., Abdelmoti, L., Jang, E. R., Vander Kooi, C. W. and Galperin, E. (2013). Functional integration of the conserved domains of Shoc2 scaffold. *PLoS ONE* **8**, e66067. doi:10.1371/journal.pone.0066067
Jin, J., Liu, J., Chen, C., Liu, Z., Jiang, C., Chu, H., Pan, W., Wang, X., Zhang, L., Li, B. et al. (2016). The deubiquitinase USP21 maintains the stemness of mouse embryonic stem cells via stabilization of Nanog. *Nat. Commun.* **7**, 13594. doi:10.1038/ncomms13594
Jindal, G. A., Goyal, Y., Burdine, R. D., Rauen, K. A. and Shvartsman, S. Y. (2015). RASopathies: unraveling mechanisms with animal models. *Dis. Model Mech.* **8**, 769-782. doi:10.1242/dmm.020339
Jindal, G. A., Goyal, Y., Yamaya, K., Futran, A. S., Kountouridis, I., Balgobin, C. A., Schüpbach, T., Burdine, R. D. and Shvartsman, S. Y. (2017). In vivo severity ranking of Ras pathway mutations associated with developmental disorders. *Proc. Natl. Acad. Sci. USA* **114**, 510-515. doi:10.1073/pnas.1615651114
Khoronenkova, S. V. and Dianov, G. L. (2013). USP7S-dependent inactivation of mule regulates DNA damage signalling and repair. *Nucleic Acids Res.* **41**, 1750-1756. doi:10.1093/nar/gks1359
Khoronenkova, S. V., Dianova, I. I., Ternette, N., Kessler, B. M., Parsons, J. L. and Dianov, G. L. (2012). ATM-dependent downregulation of USP7/HAUSP by PPM1G activates p53 response to DNA damage. *Mol. Cell* **45**, 801-813. doi:10.1016/j.molcel.2012.01.021
Kim, R. Q. and Sixma, T. K. (2017). Regulation of USP7: a high incidence of E3 complexes. *J. Mol. Biol.* **429**, 3395-3408. doi:10.1016/j.jmb.2017.05.028
Kim, R. Q., van Dijk, W. J. and Sixma, T. K. (2016). Structure of USP7 catalytic domain and three Ubl-domains reveals a connector α-helix with regulatory role. *J. Struct. Biol.* **195**, 11-18. doi:10.1016/j.jsb.2016.05.005
Kimmel, C. B., Ballard, W. W., Kimmel, S. R., Ullmann, B. and Schilling, T. F. (1995). Stages of embryonic development of the zebrafish. *Dev. Dyn.* **203**, 253-310. doi:10.1002/aja.1002030302
Kwon, Y. T. and Ciechanover, A. (2017). The ubiquitin code in the ubiquitin-proteasome system and autophagy. *Trends Biochem. Sci.* **42**, 873-886. doi:10.1016/j.tibs.2017.09.002
Li, X., Stevens, P. D., Yang, H., Gulhati, P., Wang, W., Evers, B. M. and Gao, T. (2013). The deubiquitination enzyme USP46 functions as a tumor suppressor by controlling PHLPP-dependent attenuation of Akt signaling in colon cancer. *Oncogene* **32**, 471-478. doi:10.1038/onc.2012.66
Liefke, R., Karwacki-Neisius, V. and Shi, Y. (2017). EPOP interacts with elongin BC and USP7 to modulate the chromatin landscape. *Mol. Cell* **65**, 202. doi:10.1016/j.molcel.2016.12.006
Lo, F.-S., Wang, C.-J., Wong, M.-C. and Lee, N.-C. (2015). Moyamoya disease in two patients with Noonan-like syndrome with loose anagen hair. *Am. J. Med. Genet. A* **167**, 1285-1288. doi:10.1002/ajmg.a.37053
Ma, P., Yang, X., Kong, Q., Li, C., Yang, S., Li, Y. and Mao, B. (2014). The ubiquitin ligase RNF220 enhances canonical Wnt signaling through USP7-mediated deubiquitination of β-catenin. *Mol. Cell Biol.* **34**, 4355-4366. doi:10.1128/MCB.00731-14
Motta, M., Giancotti, A., Mastromoro, G., Chandramouli, B., Pinna, V., Pantaleoni, F., Di Giosaffatte, N., Petrini, S., Mazza, T., D'Ambrosio, V. et al. (2019). Clinical and functional characterization of a novel RASopathy-causing Shoc2 mutation associated with prenatal-onset hypertrophic cardiomyopathy. *Hum. Mutat.* **40**, 1046-1056. doi:10.1002/humu.23767
Nathan, J. A., Sengupta, S., Wood, S. A., Admon, A., Markson, G., Sanderson, C. and Lehner, P. J. (2008). The ubiquitin E3 ligase MARCH7 is differentially regulated by the deubiquitylating enzymes USP7 and USP9X. *Traffic* **9**, 1130-1145. doi:10.1111/j.1600-0854.2008.00747.x
Nicklas, S., Hillje, A.-L., Okawa, S., Rudolph, I.-M., Collmann, F. M., van Wuellen, T., Del Sol, A. and Schwamborn, J. C. (2019). A complex of the ubiquitin ligase TRIM32 and the deubiquitinase USP7 balances the level of c-Myc ubiquitination and thereby determines neural stem cell fate specification. *Cell Death Differ.* **26**, 728-740. doi:10.1038/s41418-018-0144-1
Novellasdemunt, L., Foglizzo, V., Cuadrado, L., Antas, P., Kucharska, A., Encheva, V., Snijders, A. P. and Li, V. S. W. (2017). USP7 is a tumor-specific WNT activator for APC-mutated colorectal cancer by mediating β-catenin deubiquitination. *Cell Rep.* **21**, 612-627. doi:10.1016/j.celrep.2017.09.072
Pandya, R. K., Partridge, J. R., Love, K. R., Schwartz, T. U. and Ploegh, H. L. (2010). A structural element within the HUWE1 HECT domain modulates self-ubiquitination and substrate ubiquitination activities. *J. Biol. Chem.* **285**, 5664-5673. doi:10.1074/jbc.M109.051805
Pei, D. (2017). Deubiquitylating nanog: novel role of USP21 in embryonic stem cell maintenance. *Signal Transduct. Target. Ther.* **2**, 17014. doi:10.1038/sigtrans.2017.14
Pozhidaeva, A. and Bezsonova, I. (2019). USP7: structure, substrate specificity, and inhibition. *DNA Repair* **76**, 30-39. doi:10.1016/j.dnarep.2019.02.005
Rodriguez-Viciana, P., Oses-Prieto, J., Burlingame, A., Fried, M. and McCormick, F. (2006). A phosphatase holoenzyme comprised of Shoc2/Sur8 and the catalytic subunit of PP1 functions as an M-Ras effector to modulate Raf activity. *Mol. Cell* **22**, 217-230. doi:10.1016/j.molcel.2006.03.027
Sarasin, A. (2012). UVSSA and USP7: new players regulating transcription-coupled nucleotide excision repair in human cells. *Genome Med.* **4**, 44. doi:10.1186/gm343
Saridakis, V., Sheng, Y., Sarkari, F., Holowaty, M. N., Shire, K., Nguyen, T., Zhang, R. G., Liao, J., Lee, W., Edwards, A. M. et al. (2005). Structure of the p53 binding domain of HAUSP/USP7 bound to Epstein-Barr nuclear antigen 1: implications for EBV-mediated immortalization. *Mol. Cell* **18**, 25-36. doi:10.1016/j.molcel.2005.02.029
Schwertman, P., Lagarou, A., Dekkers, D. H. W., Raams, A., van der Hoek, A. C., Laffeber, C., Hoeijmakers, J. H. J., Demmers, J. A. A., Fousteri, M., Vermeulen, W. et al. (2012). UV-sensitive syndrome protein UVSSA recruits USP7 to regulate transcription-coupled repair. *Nat. Genet.* **44**, 598-602. doi:10.1038/ng.2230
Schwertman, P., Vermeulen, W. and Marteijn, J. A. (2013). UVSSA and USP7, a new couple in transcription-coupled DNA repair. *Chromosoma* **122**, 275-284. doi:10.1007/s00412-013-0420-2
Sheng, Y., Saridakis, V., Sarkari, F., Duan, S., Wu, T., Arrowsmith, C. H. and Frappier, L. (2006). Molecular recognition of p53 and MDM2 by USP7/HAUSP. *Nat. Struct. Mol. Biol.* **13**, 285-291. doi:10.1038/nsmb1067
Sieburth, D. S., Sun, Q. and Han, M. (1998). SUR-8, a conserved Ras-binding protein with leucine-rich repeats, positively regulates Ras-mediated signaling in C. elegans. *Cell* **94**, 119-130. doi:10.1016/S0092-8674(00)81227-1
Sowa, M. E., Bennett, E. J., Gygi, S. P. and Harper, J. W. (2009). Defining the human deubiquitinating enzyme interaction landscape. *Cell* **138**, 389-403. doi:10.1016/j.cell.2009.04.042
Thompson, J. W., Nagel, J., Hoving, S., Gerrits, B., Bauer, A., Thomas, J. R., Kirschner, M. W., Schirle, M. and Luchansky, S. J. (2014). Quantitative Lys-ε-Gly-Gly (diGly) proteomics coupled with inducible RNAi reveals ubiquitin-mediated proteolysis of DNA damage-inducible transcript 4 (DDIT4) by the E3 ligase HUWE1. *J. Biol. Chem.* **289**, 28942-28955. doi:10.1074/jbc.M114.573352
Tidyman, W. E. and Rauen, K. A. (2016). Pathogenetics of the RASopathies. *Hum. Mol. Genet.* **25**, R123-R132. doi:10.1093/hmg/ddw191
Tse, W. K. F., Eisenhaber, B., Ho, S. H. K., Ng, Q., Eisenhaber, F. and Jiang, Y.-J. (2009). Genome-wide loss-of-function analysis of deubiquitylating enzymes for zebrafish development. *BMC Genomics* **10**, 637. doi:10.1186/1471-2164-10-637
van der Horst, A., de Vries-Smits, A. M. M., Brenkman, A. B., van Triest, M. H., van den Broek, N., Colland, F., Maurice, M. M. and Burgering, B. M. T. (2006). FOXO4 transcriptional activity is regulated by monoubiquitination and USP7/HAUSP. *Nat. Cell Biol.* **8**, 1064-1073. doi:10.1038/ncb1469
van der Knaap, J. A., Kumar, B. R. P., Moshkin, Y. M., Langenberg, K., Krijgsveld, J., Heck, A. J. R., Karch, F. and Verrijzer, C. P. (2005). GMP synthetase stimulates histone H2B deubiquitylation by the epigenetic silencer USP7. *Mol. Cell* **17**, 695-707. doi:10.1016/j.molcel.2005.02.013
Wang, Z., Kang, W., You, Y., Pang, J., Ren, H., Suo, Z., Liu, H. and Zheng, Y. (2019). USP7: novel drug target in cancer therapy. *Front. Pharmacol.* **10**, 427. doi:10.3389/fphar.2019.00427
Xie, C.-M. and Sun, Y. (2019). The MTORC1-mediated autophagy is regulated by the FBXW7-Shoc2-RPTOR axis. *Autophagy* **15**, 1470-1472. doi:10.1080/15548627.2019.1609864

Xie, C.-M., Tan, M., Lin, X.-T., Wu, D., Jiang, Y., Tan, Y., Li, H., Ma, Y., Xiong, X. and Sun, Y. (2019). The FBXW7-Shoc2-raptor axis controls the cross-talks between the RAS-ERK and mTORC1 signaling pathways. *Cell Rep.* **26**, 3037-3050.e4. doi:10.1016/j.celrep.2019.02.052

Ye, M., Tang, Y., Tang, S., Liu, J., Wu, K., Yao, S., Sun, Y., Zhou, L., Deng, T., Chen, Y. et al. (2015). STIP is a critical nuclear scaffolding protein linking USP7 to p53-Mdm2 pathway regulation. *Oncotarget* **6**, 34718-34731. doi:10.18632/oncotarget.5303

Yi, J., Chen, M., Wu, X., Yang, X., Xu, T., Zhuang, Y., Han, M. and Xu, R. (2010). Endothelial SUR-8 acts in an ERK-independent pathway during atrioventricular cushion development. *Dev. Dyn.* **239**, 2005-2013. doi:10.1002/dvdy.22343

Young, L. C., Hartig, N., Muñoz-Alegre, M., Oses-Prieto, J. A., Durdu, S., Bender, S., Vijayakumar, V., Vietri Rudan, M., Gewinner, C., Henderson, S. et al. (2013). An MRAS, Shoc2, and SCRIB complex coordinates ERK pathway activation with polarity and tumorigenic growth. *Mol. Cell* **52**, 679-692. doi:10.1016/j.molcel.2013.10.004

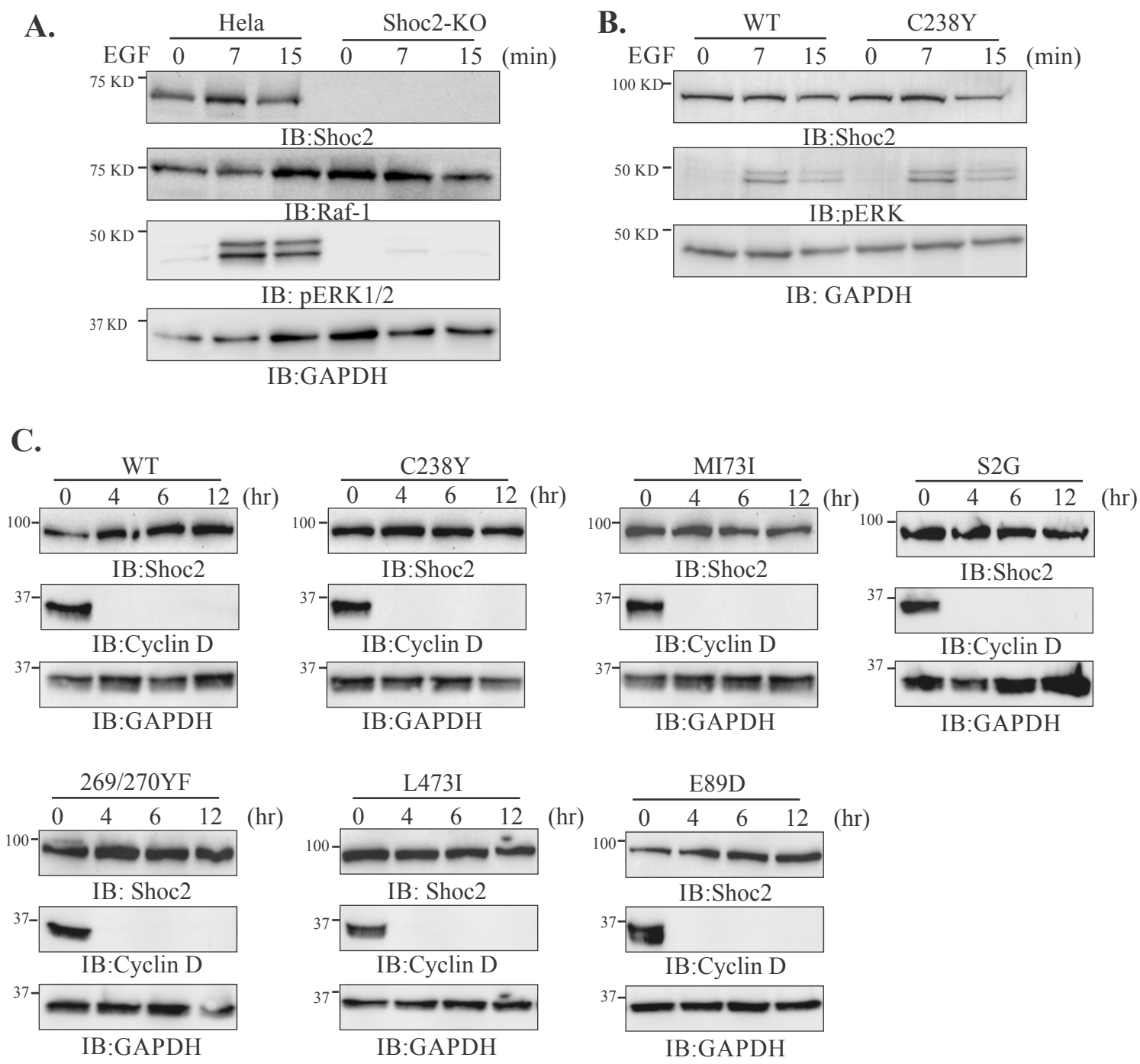

Fig. S1. Full-length Shoc2-tRFP and Shoc2-tRFP NSLAH-associated mutants have similar protein half-life.

A. Parental and CRISPR/Cas9 Shoc2 KO HeLa cells were serum-starved for 16 hr and then stimulated with EGF (0.2 ng/ml) for 7 and 15 min. Immunoblots were analyzed with anti-Shoc2, -RAF-1, -pERK1/2, and -GAPDH antibodies. The results in each panel are representative of those from three independent experiments.

B. HeLa Shoc2 CRISPR KO cells transiently transfected with the Shoc2 C238Y mutant were serum-starved for 16 hr and then stimulated with EGF (0.2 ng/ml) for 7 and 15min. Cell lysates were analyzed using anti-pERK1/2, -GAPDH and -Shoc2 antibodies.

C. CRISPR/Cas9 Shoc2 KO HeLa cells were transiently transfected with full-length Shoc2-tRFP or Shoc2-tRFP mutants. Thirty-six hours post-transfection cells were treated with 30 μM Cycloheximide for indicated times at 37°C. The lysates were probed by immuno-blotting (IB) for Shoc2, Cyclin D (half-life 30 min, experimental control) and GAPDH (loading control).

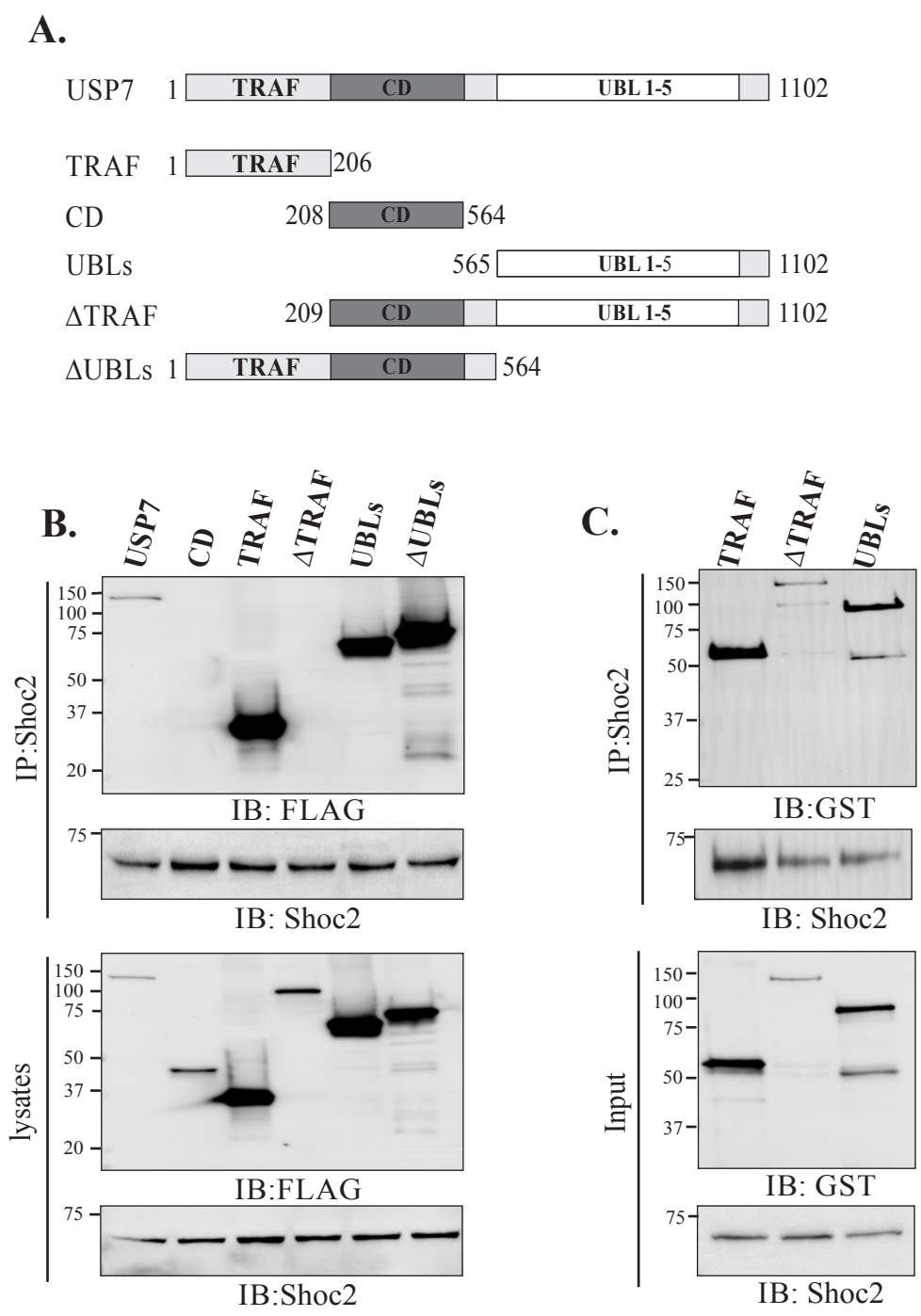

Fig. S2. Mapping the architecture of the Shoc2-USP7 complex.

A. Schematic representation of the full-length and truncated FLAG-USP7 constructs.

B. Co-immunoprecipitation studies reveal the importance of TRAF (aa1-206) and UBL1-5 (aa564-1102) domains for Shoc2 interaction in cells. The indicated constructs were expressed in 293FT cells for 48 hrs before cell lysates were immunoprecipitated with anti-Shoc2 and immunoblotted with anti-FLAG (USP7). Cell lysates were immunoblotted with anti-FLAG antibody to monitor expression of USP7 and corresponding truncated mutants used in IP panel or Shoc2 Abs to monitor expression of Shoc2.

C. Purified indicated recombinant fragments of USP7 were used in *in vitro* Shoc2-pulldown assays to determine the regions on USP7 that Shoc2 binds. GST or GST-USP7 fragments were incubated with recombinant His-Shoc2 bound to Sepharose A beads. Bound proteins were detected by anti-GST and Shoc2 immunoblotting.

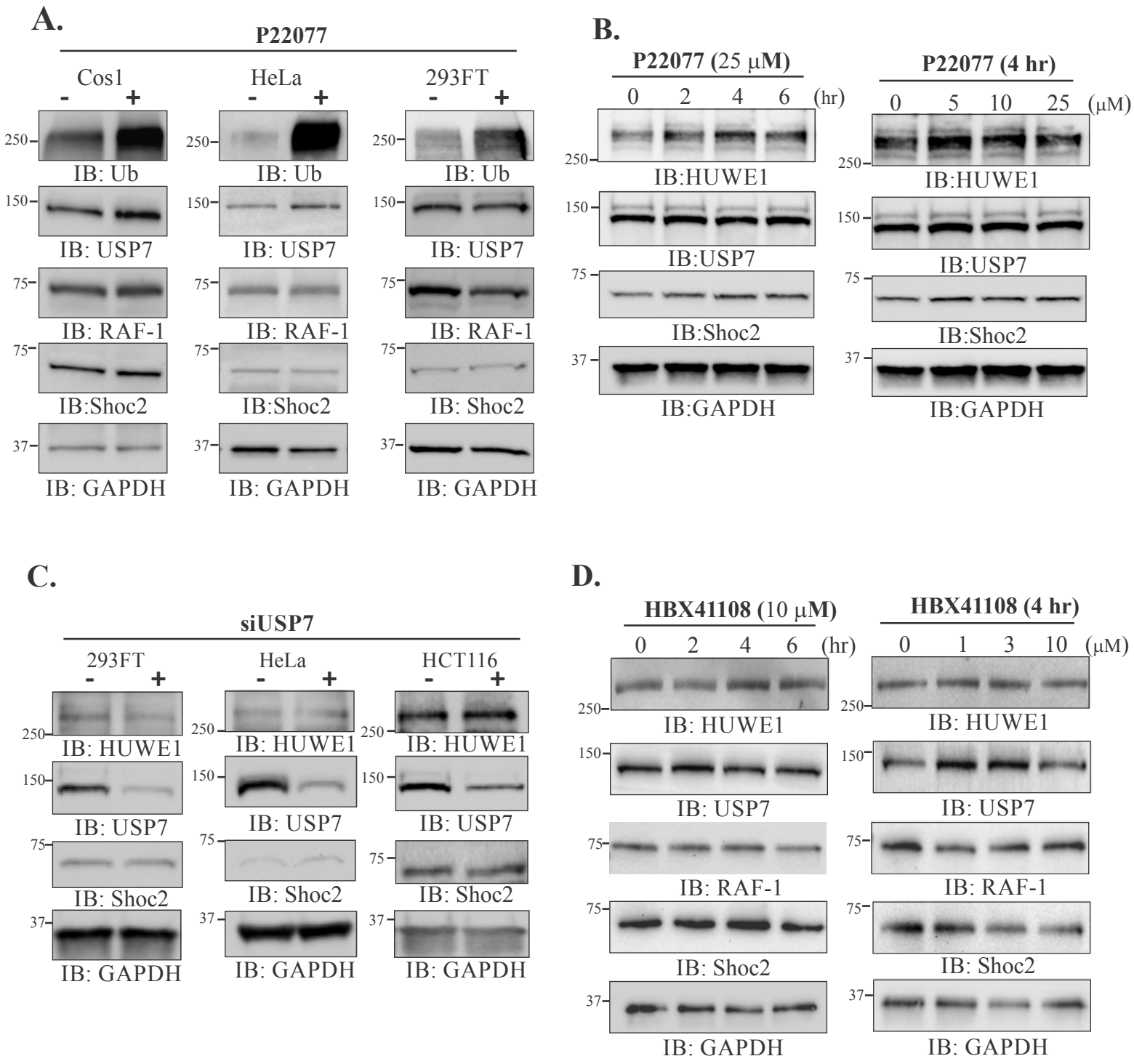

Fig. S3. USP7 does not modify levels of the proteins in the Shoc2 complex.

A. Cos-1, HeLa or 293FT cells were treated with the vehicle (DMSO) or 25 of P22077 for 4 hr. Cell lysates were analyzed using anti-Ub, -USP7, -RAF-1, -Shoc2 and -GAPDH antibodies. **B.** 293FT cells were treated with the vehicle (DMSO) or 10 μM of P22077 at the time period indicated or indicated doses of P22077. Cell lysates were analyzed using anti-HUWE1, -USP7, -Shoc2, and -GAPDH antibodies.

C. HeLa, HCT116 and 293FT cells were transiently transfected with non-targeting siRNA (siNT) or USP7 siRNA (siUSP7). Cell lysates were analyzed using anti-HUWE1, -USP7, -Shoc2 and -GAPDH antibodies.

D. 293FT cells were treated with the vehicle (DMSO) or 10 μM of HBX41108 at the time period indicated or indicated doses of HBX41108. Cell lysates were analyzed using anti-HUWE1, -USP7, -RAF-1, -Shoc2, and -GAPDH antibodies.

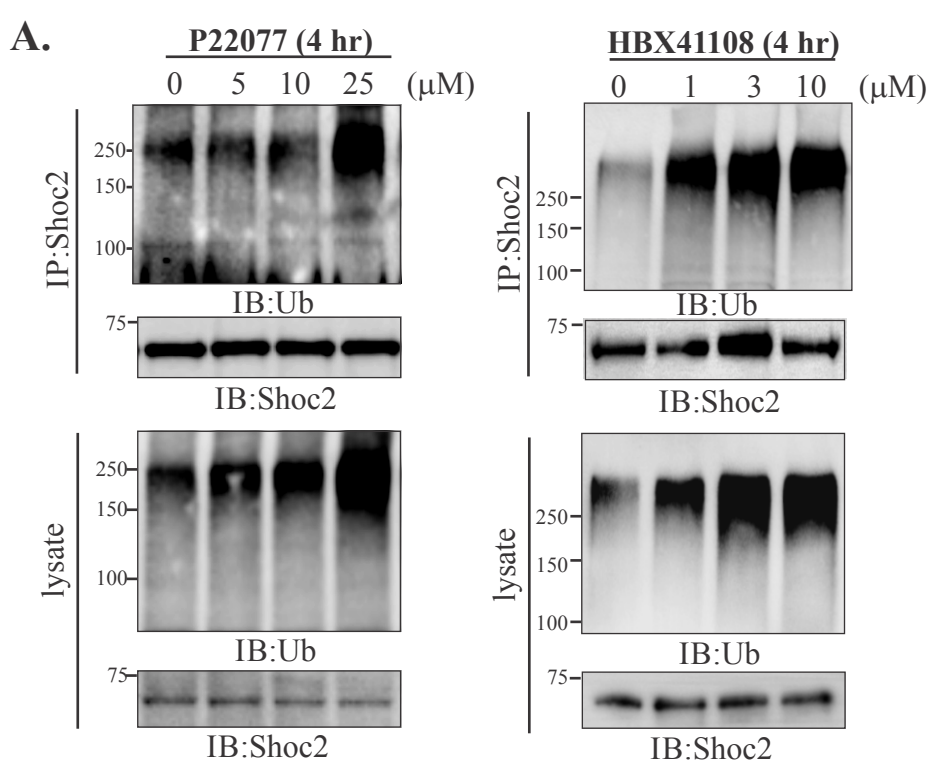

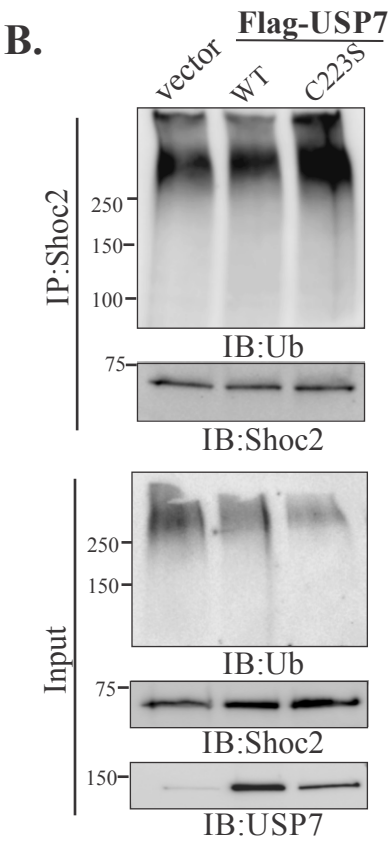

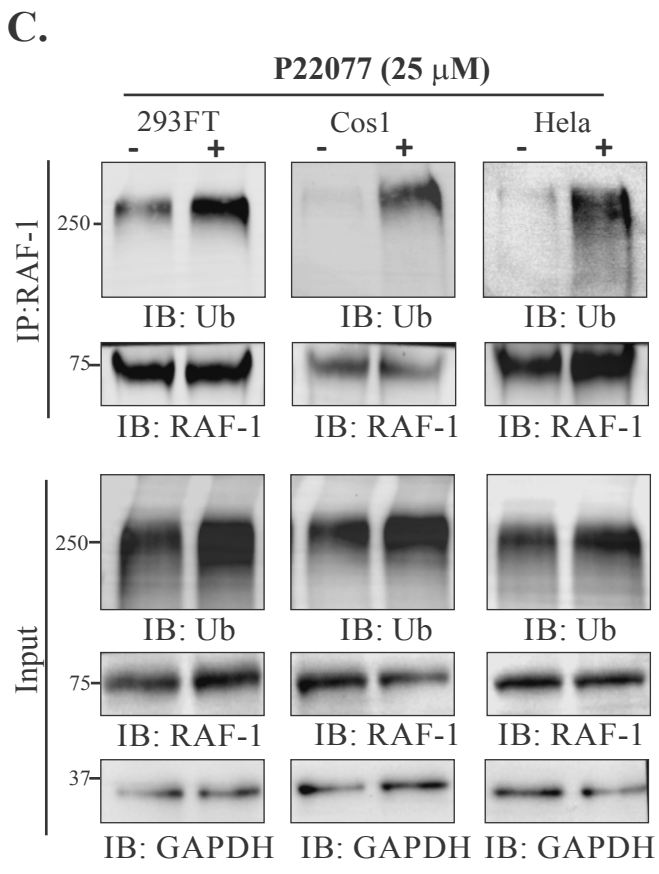

Fig. S4. USP7 does not modify levels of the proteins in the Shoc2 complex. A. Endogenous Shoc2 was immunoprecipitated from 293FT cells treated with USP7 inhibitor P22077 or HBX41108. Shoc2 ubiquitination was detected by immunoblotting using anti-ubiquitin (Ub) antibody. The immunoprecipitates and cell lysates were analyzed by immunoblotting with using anti-Ub, and -Shoc2 antibodies. The results in each panel are representative of those from three independent experiments.

B. 293FT cells were transfected with WT FLAG-USP7 or FLAG-USP7 with the C223S substitution. Shoc2 was immunoprecipitated using anti-Shoc2, and Shoc2 ubiquitination was detected with anti-Ub antibodies. Cell lysates were analyzed using anti-Ub, -USP7 and -Shoc2 antibodies.

C. Endogenous RAF-1 was immunoprecipitated from 293FT, Cos1 or HeLa cells treated with USP7 inhibitor P22077. RAF-1 ubiquitination was detected by immunoblotting using anti-ubiquitin (Ub) antibody. The immunoprecipitates and cell lysates were analyzed by immunoblotting with using anti-Ub, -RAF-1 and GAPDH antibodies. The results in each panel are representative of those from three independent experiments.

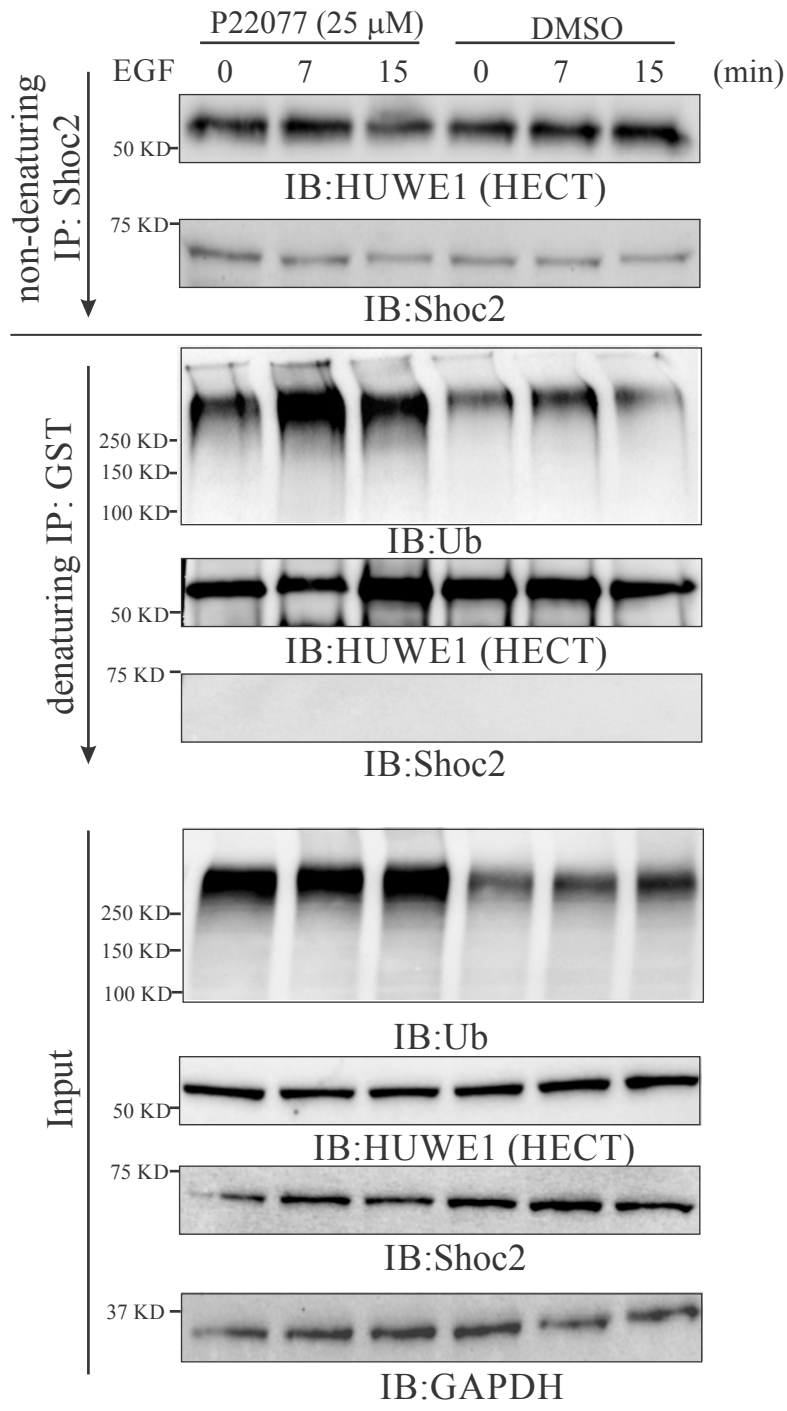

Fig. S5. USP7 regulates ubiquitination of Shoc2- bound HECT domain of HUWE1.

293FT cells were transiently transfected with GST-tagged HECT domain of HUWE1. 48 hours after transfections cells were serum-starved for 16 hr, treated with 25 μM of P22077 for 4 hr and then stimulated with EGF (0.2 ng/ml) for 7 and 15min. Endogenous Shoc2 was precipitated under non-denaturing conditions. Shoc2 immuno-precipitates were then denatured and subjected for immunoprecipitation using anti-HUWE1 antibody. HUWE1 ubiquitination was detected with anti-ubiquitin (Ub) antibody. Immunoblots were analyzed with anti-Shoc2, - HUWE1, -Ub, and GAPDH antibodies. The results are representative of at least three independent experiments.

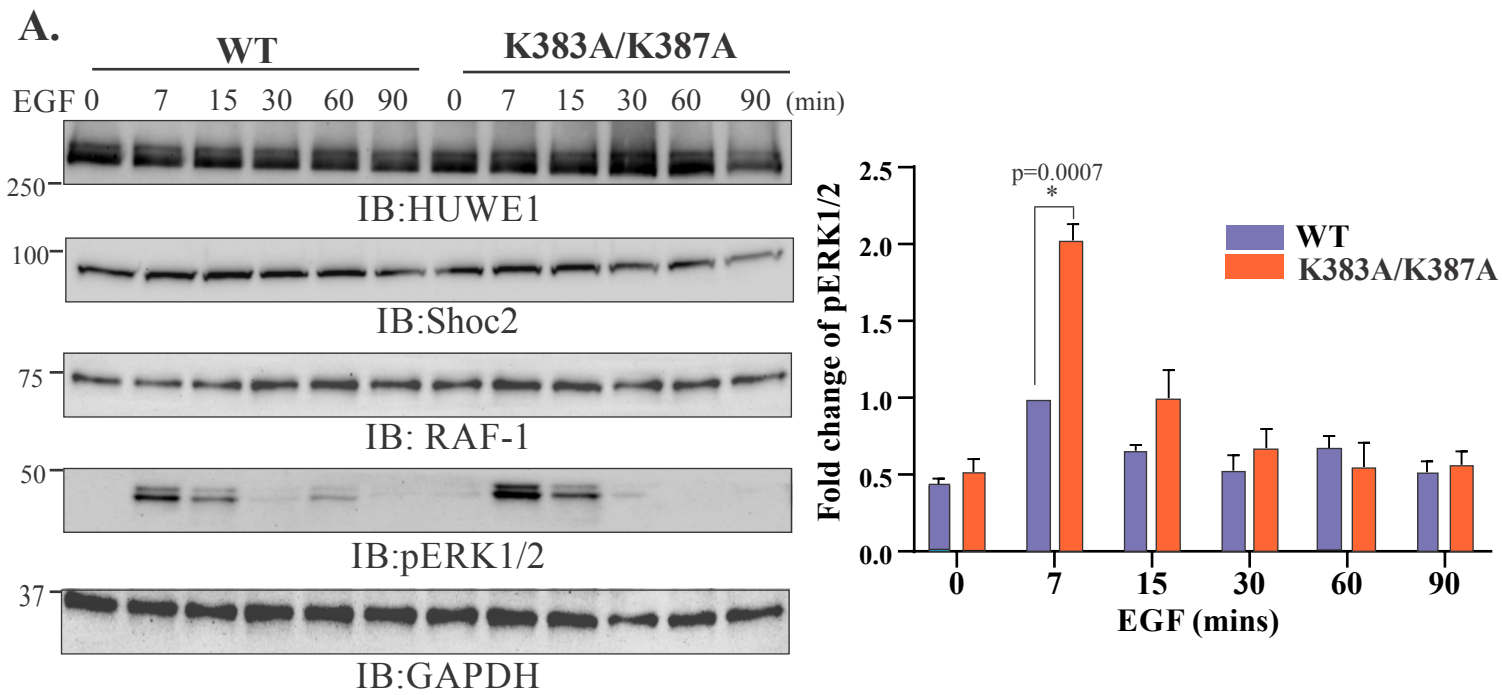

Fig. S6. ERK1/2 pathway activation in cells expressing USP7-binding deficient mutants of Shoc2.

HeLa cells were transfected with WT Shoc2-tRFP, Shoc2 (K383/387A) (**A**) or Shoc2 (K22/26A) (**B**) mutants respectively. Cells were serum-starved for 16 hr and then stimulated with EGF (0.2 ng/ml). Immunoblots were analyzed with anti -HUWE1, -Shoc2, -RAF-1, -pERK1/2 and -GAPDH antibodies. Bars represent the mean amount of pERK1/2 normalized to the total amount of GAPDH in arbitrary units ± S.E. (n=3) (p<0.0007 (*7 min K383/387A*), by Student's *t*-test and p<0.0488 (*7 min K22/26A*), by Student's *t*-test). The results in each panel are representative of those from three independent experiments.

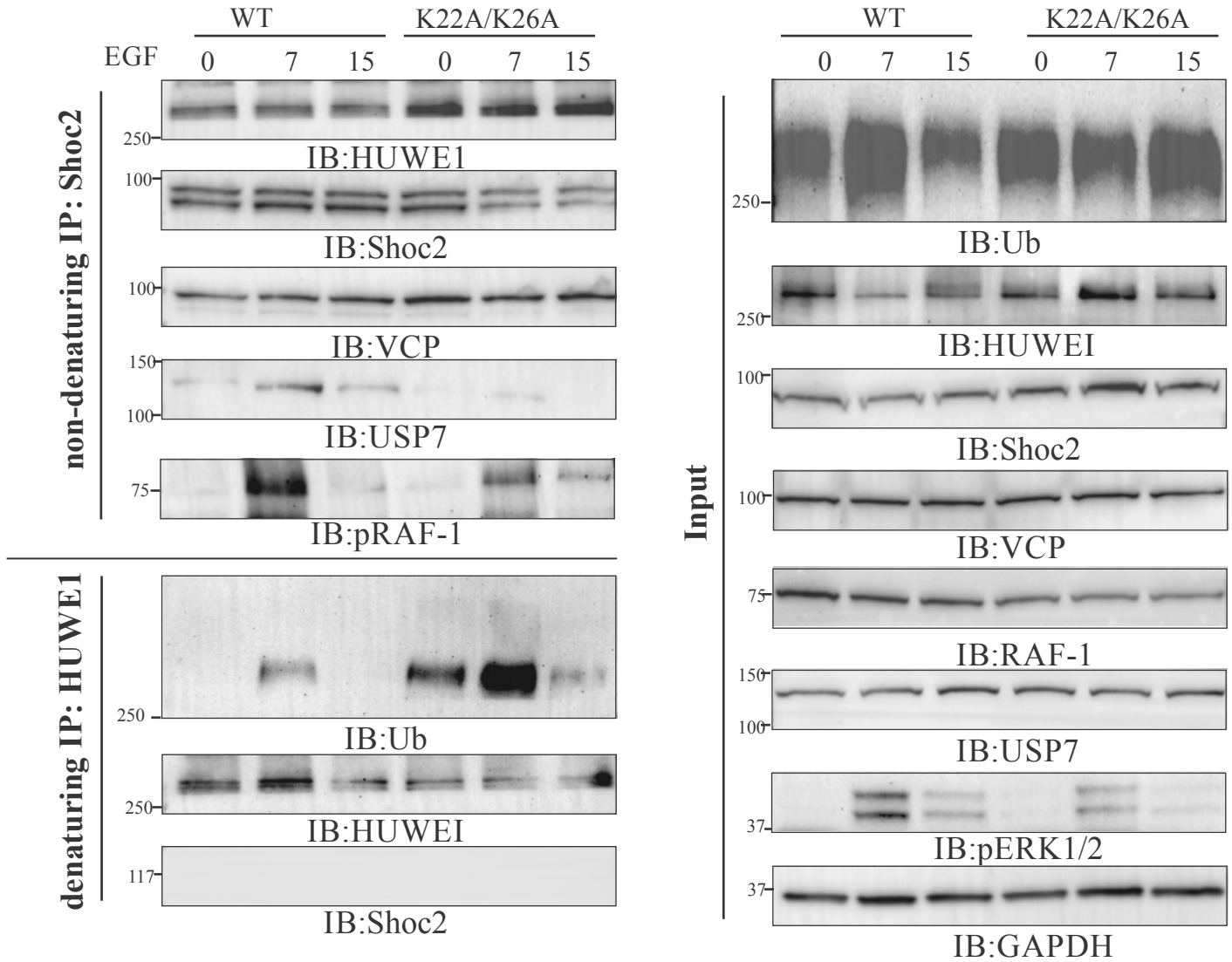

Fig. S7. USP7 regulates ubiquitination of Shoc2- bound HUWE1.

HeLa Shoc2 CRISPR KO cells expressing WT Shoc2-tRFP or the Shoc2 mutant K22/26A were serum-starved for 16 hr and then stimulated with EGF (0.2 ng/ml) for 7 and 15min. Endogenous Shoc2 was precipitated under non-denaturing conditions. 50% of Shoc2 immunoprecipitates were analyzed with anti-HUWE1, -VCP, -Shoc2, -USP7 and RAF-1 antibody. The rest of Shoc2 immunoprecipitates were then denatured and subjected for immunoprecipitation using anti-HUWE1 antibody. Ubiquitination was detected with anti-ubiquitin (Ub) antibody. Immunoblots were analyzed with anti-Shoc2, -Ub and -HUWE1 antibodies. Cell lysates were probed with anti-Ub, -HUWE1, -VCP, -Shoc2, -USP7, pERK1/2, GAPDH and RAF-1 antibody. The results in each panel are representative of those of at least three independent experiments.

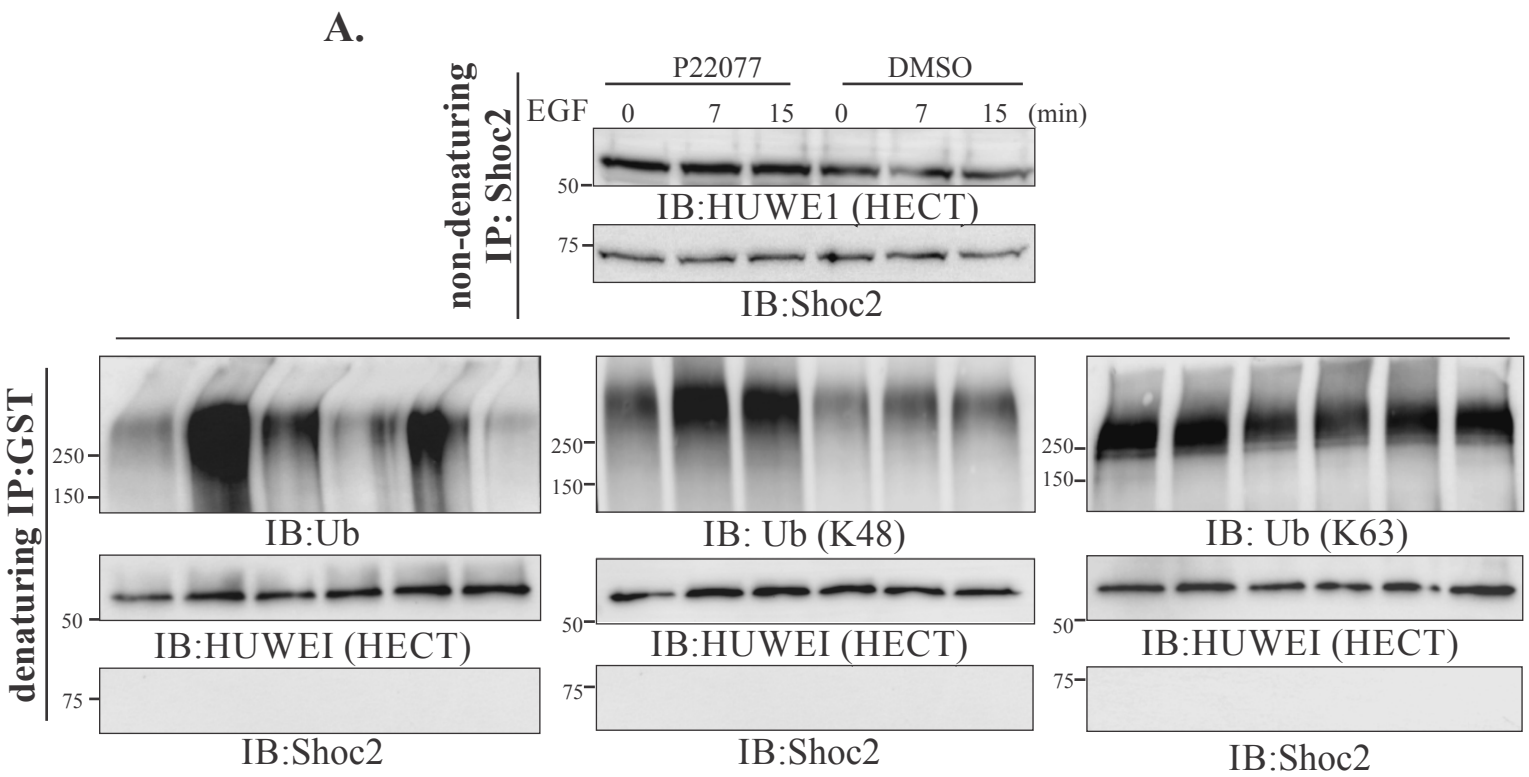

Fig. S8. USP7 modulated K48 linkages on Shoc2-bound HUWE1 in cells stimulated with EGF.

A. 293FT cells were transfected with GST-tagged HECT domain of HUWE1. Endogenous Shoc2 was precipitated under non-denaturing conditions from cells treated with P22077 (25μM) for 4 hours. Shoc2 immuno-precipitates were analyzed with anti-HUWE1 and Shoc2 antibody. Shoc2 precipitates were then denatured and subjected for immunoprecipitation using anti-HUWE1 antibody. Ubiquitination was detected with anti-K48 ubiquitin (K48), -K63 ubiquitin (K63) or -Ub antibody. Cell lysates were probed with anti-HUWE1, -Shoc2, and -GAPDH antibody. The results in each panel are representative of those of at least three independent experiments.

B. The mean amount of Ub normalized to the total amount of HECT ubiquitination at 0 min ± SE from three experiments is presented on the graph. The results in each panel are representative of those from three independent experiments.

Table 1	Mutation Summary and Clinical Phenotypes of Seven Individuals with Shoc2 mutations						
	Subject Number						
DECIPHER ID	1 (254516)	2 (259095)	3 (3284096)	4 (287439)	5 (287504)	6 (296587)	7 (318097)
Characteristic							
Sex	M	M	M	M	M	F	M
Age	>1	12	3	3	3	18	?
Mutation type	Del	missense c.A4>G p.S2G	missense c.G713>A p.C238Y	missense c.G267>C p.E89D	missense c.T1417>A p.L473I	missense c.A4>G p.S2G	missense c.A4>G p.S2G
Inheritance	de novo	de novo	UN	UN	maternally inherited	de novo	UN
Genomic size	2.19 Mb	1b	1b	1b	1b	1b	1b
Genes affected (n)	10	1	4	2	4	2	1
Symptoms							
Heart defects	V			V	V	V	
Hair			V		V	V	
Short stature		V				V	
Intellectual disability		V	V	N/A	V	V	V
Skin tags	V		V				

b, bases; **Del**, deletion; **F,** female; **M**, male; **Mb**, megabases; **N/A**, not applicable; **UN,** unknown; **v,** present.

Table 2: Supplemental Clinical Notes
DECIPHER ID 254516 – (deletion 2.19 Mb)
Abnormal heart morphology, Abnormality of the kidney, Coarctation of aorta, Preauricular skin tag, Sacral dimple, Single transverse palmar crease, Skin tags, Tricuspid regurgitation
DECIPHER ID 259095 - (SNV A>G)
Abnormal fundus morphology, Abnormality of dental morphology, Bilateral ptosis, Epistaxis, Highly arched eyebrow, Long palpebral fissure, Moderately short stature, Specific learning disability.
DECIPHER ID 284096 - (SNV G>A)
Absent septum pellucidum, Clinodactyly of the 5th finger, Numerous nevi, Optic atrophy, Septo-optic dysplasia, Short distal phalanx of finger, Skin tags At age 8 years old: Septo-optic dysplasia with right optic nerve hypoplasia, absent septum pellucidum, normal pituitary and corpus callosum, visual impairment of unknown cause. Previous suboptimal Synacthen test, now normal pituitary function and Synacthen Hypermobility. Behavioral problems and mild learning difficulty very white/blond hair and a small black hair patch a number of cutaneous pink/brown nevi including on his scalp and which appear to be growing both in number and in dimensions.
DECIPHER ID 287439 - (SNV G>C)
Penile hypospadias, Talipes, Tetralogy of Fallot
DECIPHER ID 287504 - (SNV T>A)
Bilateral conductive hearing impairment, Brachycephaly, Bruxism, Cleft palate, Clinodactyly of the 5th finger, Developmental regression, Gastroesophageal reflux, Gastrostomy tube feeding in infancy, Global developmental delay, Micropenis, Mitral regurgitation, Recurrent lower respiratory tract infections, Seizures, Talipes equinovarus, Upslanted palpebral fissure.
DECIPHER ID 296587 - (SNV A>G)
Atrial septal defect, Bilateral ptosis, Broad neck, Chronic otitis media, Delayed puberty, Downslanted palpebral fissures, Dry skin, Feeding difficulties in infancy, Fine hair, Gray matter heterotopias, Intellectual disability, moderate, Pulmonic stenosis, Severe short stature. At age 23 patient had pulmonary stenosis and an ASD. She has longstanding short stature adult height around 135cm. Very significant learning problems – very limited reading and writing and needs supervision in daily activities.
DECIPHER ID 318097 - (SNV A>G)
Intellectual disability.